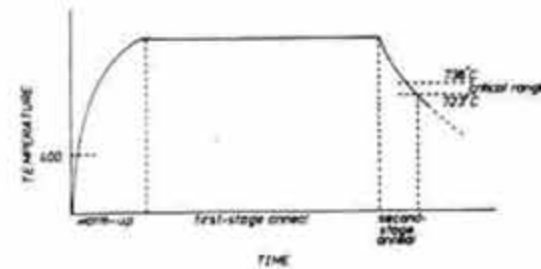


**East Asian Institute
Occasional Papers
4**

**Toward the Reconstruction of
Ancient Chinese Techniques
for the Production of
Malleable Cast Iron**



**East Asian Institute
University of Copenhagen
1989**

**East Asian Institute
Occasional Papers
4**

Edited by
Søren Egerod

Donald B. Wagner

**Toward the Reconstruction of
Ancient Chinese Techniques
for the Production of
Malleable Cast Iron**

East Asian Institute
University of Copenhagen
1989

East Asian Institute
Occasional Papers

East Asian Institute
University of Copenhagen
Njalsgade 80
DK-2300 Copenhagen S
Denmark

The Chairman of the Institute
is *ex officio* editor of the
Occasional Papers.

Set in 10 point Palatino using
hardware and software provided by
The Institute for Humanistic
Informatics, University of
Copenhagen

Printed by
Det Humanistiske Fakultets Repro-afdeling
v/ Willy Christensen

© Donald B. Wagner 1989

ISSN 0903-6822

Toward the reconstruction of ancient Chinese
techniques for the production of malleable cast iron

Donald B. Wagner

This paper was originally presented at the Third International Conference on the History of Chinese Science, Beijing, 20-25 August 1984. In October 1984 a revised version was submitted for publication in the conference proceedings. It now seems that the publication of the proceedings has been postponed indefinitely, and I am therefore pleased to have the opportunity to publish it in the East Asian Institute's new series of occasional papers. Minor revisions have been made throughout the paper, and the mathematical appendix (section 7) has been entirely rewritten.

1. Introduction

Cast iron is generally rather brittle, but annealing a casting at a high temperature for a long period of time (typically 850-1050°C for several days) can greatly improve its strength and toughness. The product is called *malleable cast iron*. This process provides a cheap and only slightly inferior substitute for steel in many applications in which ordinary cast iron (at least before modern advances) is not sufficiently strong and tough.

An example can be seen in figure 1, which shows two gads from an ancient Chinese copper-mine site. It can be seen at a glance that this type of mining implement must be subjected to extremely hard treatment, being hammered into cracks in the rock. Ordinary white or grey cast iron would surely break. Yet the heads of these implements are of cast iron; metallographic examination shows that they were toughened by malleablizing annealing (Hua Jueming 1982: 4-5, item no. 20).

Studies by Chinese metallurgists and archaeologists in the past three decades have shown that malleable cast iron was widely used in China at least as early as the third century B.C., and continued in use until perhaps the sixth century A.D., after which it seems to have fallen out of use and been forgotten. It was reintroduced in China from the West in the early twentieth century. A very useful survey of 52

ancient Chinese malleable cast iron artifacts has been published by Prof. Hua Jueming (1982).¹

In the West the technique is much later. It was patented in England by Prince Rupert (Ruprecht von der Pfalz, 1619–1682) in 1670,² and was first studied systematically by René Antoine Ferchault de Réaumur (1683–1757); Sisco and Smith (1956) have published an English translation of Réaumur's study, which was first published in 1722.

Nothing is known of what Prince Rupert intended to use his patented process for, but Réaumur's aim was primarily to soften the surface of a casting so that it could be finished by engraving and filing; figure 2 shows some of the types of casting he was concerned with. It was only later, perhaps in the early nineteenth century, that the possibility of cheap mass-produced implements with reasonable mechanical properties was exploited. Figure 3 shows some typical examples of malleable castings produced in California in 1884; here malleable cast iron is obviously a cheap substitute for wrought iron worked by smiths.

The history of malleable cast iron in the West has not yet been written. Some early descriptions of contemporary malleable foundry practice are given by Strickland (1826), Terhune (1871), Rott (1881), and Guédras (1927–28). Voye (1914), Vogel (1918–20), Maurmann (1923), and Schütz and Stotz (1930: 1–48) give some useful historical notes, mostly on developments in Germany. Deprez (1930) and Davis (1898) discuss early developments in Belgium and the United States respectively. It appears that the technique first became industrially important in the early nineteenth century, in Britain, and spread from there to continental Europe. The period of greatest relative importance of malleable cast iron may have been about the end of the nine-

¹Metallographic studies of ancient Chinese iron artifacts available in Western languages include: Pinel et al. 1938; Lu Da 1965; Henger 1970; Ye Jun 1975; KG 1975.4: 241ff; WW 1976.8: 52ff; WW 1978.10: 44ff; Du Fuyun 1981; Rostoker et al. 1984.

²Prince Rupert's original patent was granted on 6 May 1670, but apparently it was never published. It is quoted in Patent no. 164 for 1671, with all technical details omitted. Patent no. 161 for 1670 transfers the rights to this patent from Prince Rupert to "Hartgill Baron Edmund Hampden & Thomas Stringer"; but Patent no. 164 for 1671 assigns the same rights to the King, Charles II. Patent no. 165 for 1671 is a grant to Prince Rupert and two representatives of the Crown of the right to administer oaths of secrecy to workmen employed in the application of the original patent. These three patents were published at the Great Seal Patent Office, Holborn, 1857; I am grateful to Dr. Michael Salt for tracking them down for me. On other early English patents see Lohse 1910: 102; Vogel 1918: 1101–1102; Schubert 1957: 270–271.



Figure 1 Two gads from the ancient copper-mine site at Tonglushan in Daye County, Hubei (Hua Jueming 1982, plate 1.2). Tentatively dated to the fourth or third century B.C.

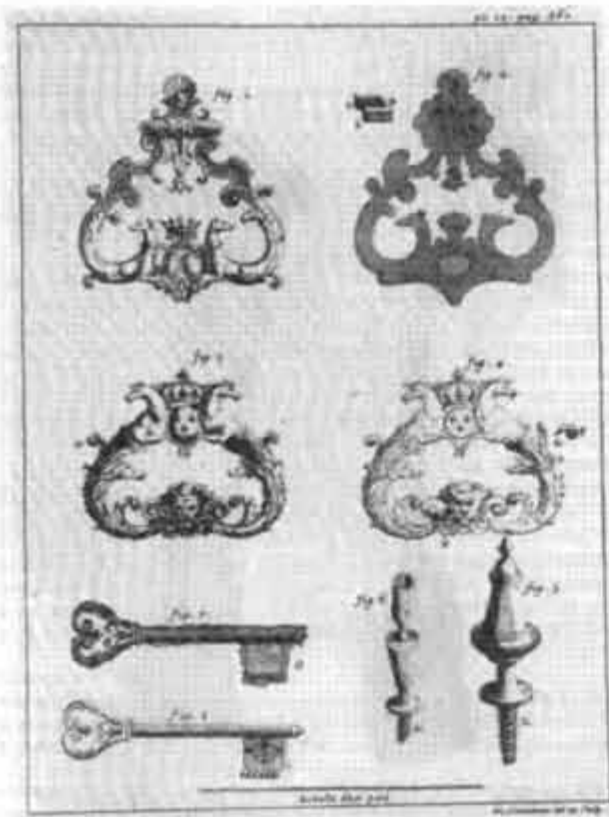


Figure 2 An illustration from Réaumur's *L'art de convertir le fer forgé en acier, et l'art d'adoucir le fer fondu, ou de faire des ouvrages de fer fondu aussi fini que de fer forgé*. Paris 1722. 1-4: door knockers; 5: part of a fire grate; 6: upright part of a candlestick; 7-8: a key before and after finishing. These are all of malleable cast iron except for the parts marked A, B, C, G, L, and M, which are cast-in pieces of wrought iron. The scale shows one foot, here equal to ca. 32.5 cm (Sisco & Smith 1956: 431).

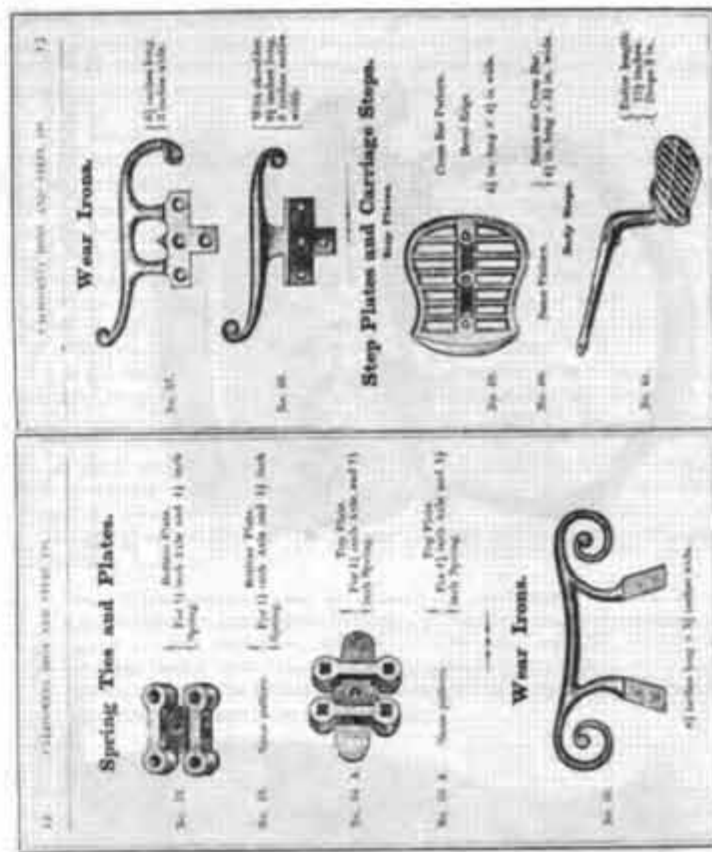


Figure 3 Two pages from illustrated catalogue of malleable iron castings made by the California Iron and Steel Company, San Francisco 1884, preserved in the Bancroft Library, University of California, Berkeley, California, U.S.A.



Figures 4 and 5 Japanese cast-iron vase and tea-kettle. The decoration is not cast-in, as is more usual in such pieces, but incised and inlaid after a preparatory surface-decarburation (Rein 1886, plate XVII & p. 518).



teenth century, after which the falling cost of steel and the rising cost of fuel made it a less attractive alternative; but malleable cast iron is still very important in industry today. World production of malleable castings is well over a million tons per year.

It was noted above that malleable cast iron appears to have gone out of use in China by about the sixth century A.D. A very similar technique, however, was used in Japan until late in the nineteenth century. It was used, as in Réaumur's case, for surface-softening cast-iron tea kettles and other art objects preparatory to decoration and inlaying; two examples are shown in figures 4 and 5. J. J. Rein's brief description of the technique, published in 1886, is reproduced in the box on p. 10. Whether the technique was learned from China, or reinvented in Japan, is not clear. From the description it seems too time-consuming for mass production of implements as in ancient China.³

A question which will require further research is whether the European development of malleable cast iron owed anything to a knowledge of this Japanese technique, which might for example have been brought back by early Dutch merchants. (Prince Rupert grew up in Holland and was educated in Leiden; see Vogel 1918: 1101–1102.) The Japanese technique was known in Europe as early as 1734. Emanuel Swedenborg has, in his *De ferro*, a very short chapter on siderurgical techniques in "the Indies", a term which for him includes all of Asia. Here he writes:⁴

There is also a tradition that the Chinese and the Japanese know an art of bringing iron to a high degree of softness, so that it can receive impressions of figures as easily as lead can; and that they later can give it again its original hardness. Becher⁵ seems also to boast that he could do this; this is why I mention the matter. In the following you will learn of the method described by the ingenious Mr. Réaumur for softening iron.

³It is also interesting to note a statement by Sir John Barrow, who visited China as a member of Lord Macartney's mission, 1793–1794: "their cast-iron wares appear light and neat, and are annealed in heated ovens, to take off somewhat of their brittleness..." (Barrow 1804: 299). The passage in which he states this appears largely to be based on an account by a member of the same mission, Dr. Hugh Gillan, of "the state of medicine, surgery and chemistry in China" (published by Cranmer-Byng 1962: 279ff), but Gillan does not mention the annealing of cast iron.

⁴Swedenborg 1734: 194; translated from the Swedish translation, Sjögren 1923: 230; note also the French translation, Swedenborg 1762: 115–116.

⁵Johann Joachim Becher (d. ca. 1685), a German alchemist and political economist. He mentions Prince Rupert's invention briefly in a book entitled *Nährliche Weisheit und weise Narrheit*, published in 1682 (Vogel 1918: 1101).

J. J. Rein's description of a traditional Japanese process of malleablizing annealing

More surprising than the inlaid work on the forged iron armour and the weapons, is its direct employment on cast-iron Tetsu-bin,^a vases and other articles. As is well known, the cast iron cannot, on account of its hardness and brittleness, be worked with the hammer, chisel and burin. The way in which these properties are lessened by the reduction of the carboniferous contents has been observed by Lehmann and Wagener in Kiôto.^b It is a peculiar decarburising process, by which the kettle or pot receives a structure like to that of soft iron or steel, and can then be treated in the same way as in the Zogan^c-work on forged iron.

The process of decarburisation of the surface is called Yakeru^d (to burn), and is performed with primitive apparatus. Old damaged rice kettles out of which the bottom has been knocked serve as ovens. These are plastered over on the inside with a fire clay (Oka-saki-tsuchi^e and sand mixed in equal parts), so that a cylindrical space of the size of the hole in the bottom, remains open. The Kama^f or kettle thus prepared, is turned over upon a thick plate or slab, three or four centimeters thick, made out of the same fire-proof material, which serves as a grate, and is perforated like a sieve for this purpose. In order to give this plate greater firmness, it is bound around with an iron band. The holes have a width of about 1.5 centimeters. In order to give the air free play, several stones are laid under the edge of the slab. Then the Tetsu-bin to be burned, whose outside has been carefully cleaned beforehand from dust and sand, is placed in the Kama, directly on the grate.

The difference in size between the Kama and the Tetsu-bin must be such that a space of at least five centimeters remains open around the latter. This open space is then filled with the best charcoal in pieces the size of a nut, till the Kama is filled to the rim, when the coal is kindled.

In order to increase the draught, two or three Kamas filled in the same way are set one over the other, forming a kind of chimney. When the coals have ceased glowing, others are put in, and when the second instalment is burned out, the Tetsu-bin are taken out and turned upside down (with the opening underneath), set again in the Kama and burned twice in this position. Under favourable circumstances, the surface is now sufficiently soft and tough, as is ascertained with a file. It is often the case that the furnace must be heated ten times. After the cooling the decorations are then carved as in forged iron, without danger of breaking the edges, or recoil of the burin.

(Rein 1886: 518-520; translation Rein 1889: 434-435; notes added)

^a 鉄瓶, "iron kettle"; ^b Kyôto 京都; ^c 象眼; ^d 焼ける; ^e 岡崎土; ^f 釜, "kettle", or 窯, "oven".

What was Swedenborg's source for this information? Did it give any technical details? Could Prince Rupert have seen it before 1670? Further research will be needed to answer these questions, but it seems quite possible that the development of malleable cast iron in Europe may have been inspired by a knowledge of the Japanese technique.

Metallographic studies of ancient Chinese malleable cast iron artifacts provide a basis on which it should, in principle, be possible to say in considerable detail how any particular artifact was annealed, including both temperature and time. This information should be interesting both to historians of technology and to economic historians.

The rest of this paper is concerned with the methodology of deriving such information from the metallographic data. Section 2 introduces the most important technical concepts; section 3 considers briefly the simplest case, in which the precipitation of graphite is not involved; section 4 considers the problems presented by the general case, in which graphite precipitation does occur during the anneal; and section 5 describes some preliminary experimental work on these problems.

2. Technical introduction

The following brief introduction will serve to remind metallurgists of some technical facts of which they are already aware. Space considerations preclude giving a basic introduction which would be of more use to non-metallurgists.

— An essential fact which has wide-ranging consequences for cast-iron technology is that iron-carbon alloys are governed by two related but distinct phase systems, the *metastable* iron-cementite (Fe_3C) system and the *stable* iron-graphite system (see e.g. M. Hansen 1958: 353-365). At low carbon contents the metastable system is very stable, and graphite is almost never found in steel, but in cast iron, with typically 2.5-4% carbon, both systems are important.

When molten cast iron is poured into a mould it may solidify according to the metastable system, in which carbon is in combination with iron in cementite, or according to the stable system, in which the carbon is in the form of graphite. The resulting castings are called *white* and *grey* respectively; the names come from the appearance of the fracture. (An intermediate possibility is *mottled* cast iron; here some of the carbon is in combination with iron and some is in the form of graphite.)

Table 1 Chemical analyses of some ancient Chinese cast-iron artifacts.

no.	implement type	provenance	date	C %	Si %	Mn %	S %	P %	state	No. in Hua Jueming's table (1982: 4-5)
1	gad-head	Tonglúshan	-4th/-3rd century	0.7-2.5	0.13	0.05	0.016	0.108	annealed	19
2	hexagonal hoe-head	-	-	0.07-2.98	0.08	0.01	0.006	0.10	-	20
3	hammer-head	-	-	4.3	0.19	0.05	0.019	0.152	as cast	-
4	鉞	Mancheng	-113	4.05	0.018	0.03	0.063	0.217	-	-
5	mattock-head	Tieshenggou	-1st century	1.98 2.69	0.16 0.197	0.04 0.06	0.048 0.055	0.297 0.30	annealed	13
6	pig iron	-	-	4.12	0.27	0.125	0.043	0.15	as cast	-
7	-	Guxingzhen	-1st/+2nd century	4.0	0.21	0.21	0.091	0.29	-	-
8	mould for ploughshare-cap	Mianchi	-	2.31	0.21	0.19	0.031	0.38	-	-
9	ploughshare-cap	-	-	4.47	0.06	0.04	0.028	0.24	-	-
10	axehead	-	-	0.87	0.69	0.25	0.024	0.27	annealed	49

11	sickle-blade	Mianchi	-1st/+2nd century	0.57	0.21	0.14	0.019	0.34	annealed	44
12	anvil	-	-2nd/+4th century	4.15	0.04	0.02	0.031	0.34	as cast	-
13	mould for ploughshare-cap	-	-	4.40	0.10	0.11	0.029	0.24	-	-
14	axehead	-	-	0.24	0.16	0.41	0.014	0.14	annealed	45
15	mould for axehead	-	+3rd/+4th century	3.46	0.07	0.05	0.028	0.38	as cast	-
16	axehead	-	-	0.87	0.05	0.60	0.011	0.14	annealed	47
17	-	-	-	0.29	0.10	0.58	0.011	0.11	-	48
18	-	-	-	0.6-0.9	0.16	0.05	0.020	0.11	-	15

Only a small fraction of the cast-iron artifacts whose microstructures have been examined have also been analyzed chemically. The table gives all of the published analyses which I know of; it seems likely that these analyses give a reasonably representative sampling of ancient Chinese cast iron in general.

Provenance: Nos. 1-3 are from the ancient copper-mine site at Tonglúshan, Daye County, Hubei 湖北大冶铜绿山. No. 4 is from the tomb of Liu Sheng 刘胜 (died 113 B.C.) in Mancheng, Hebei 河北满城. Nos. 5-6 are from the Han ironworks site at Tieshenggou in Gongxian County, Henan 河南巩县铁生沟.

No. 7 is from the Han ironworks site at Guxingzhen in Zhengzhou, Henan 河南郑州古荥镇. Nos. 8-18 are from a buried scrap-heap excavated in Mianchi County, Henan 河南浚县.

Sources: Hua Jueming (1982: 4-5) lists all of these artifacts which were found to have been annealed, and gives brief descriptions of the microstructures; see the last column of the table. Other sources are: Nos. 1-3, Ye Jun 1975: 19-21; no. 4, Li Zhong 1975: 8; no. 5, published by Hua Jueming only; nos. 6-7, KGXB 1978.1: 10; nos. 8-18, WW 1976.8: 52.

Cementite is extremely hard and brittle. A white iron casting with 4% carbon consists of 54% cementite and 46% pearlite, which is itself rather hard; the result is that white cast iron is also hard and brittle: it is harder than quartz. In modern industry white cast iron is used in a few applications in which abrasion resistance is important, but its chief use is as an intermediate stage in the production of malleable castings.

Graphite, on the other hand, is close to being the softest mineral known. A grey iron with 4% carbon by weight is 13% graphite by volume. The graphite is in the form of numerous microscopic flakes in a matrix of ferrite (sometimes pearlite), which is soft. Therefore grey cast iron is soft, but it is brittle because the graphite flakes, having no strength, act as internal cracks from which fractures can propagate. Grey cast iron is nevertheless an extremely useful material: it is easy to cast (because the low density of graphite almost compensates for shrinkage of the iron matrix in the mould), and it is strong enough for a wide range of applications.⁶

Whether an iron casting solidifies white or grey depends on numerous factors, the most important of which are the cooling rate in the mould and the silicon content of the iron. A low cooling rate, or a high silicon content, favours the stable iron-graphite system and therefore solidification as grey cast iron. In modern foundry practice sand moulds give a relatively low cooling rate. Grey iron contains typically 2% silicon and white iron 1% silicon.

Table I gives chemical analyses of a selection of eighteen ancient Chinese cast iron artifacts. One of these has 0.69% Si; the rest have silicon contents in the range 0.02–0.27%. Because of this extremely low silicon content, ancient Chinese cast iron is nearly always white-cast. A few grey-cast implements have been found; these may have been cast in pre-heated massive ceramic moulds to give the slow cooling necessary for the production of grey castings with such low silicon content.

Malleable cast iron is made by casting the product in white cast iron, then annealing it for an extended period. In general it has much better mechanical properties than grey iron. Either or both of two independent mechanisms may be involved: *decarburization* and *graphitization*.

If the casting is annealed in an oxidizing atmosphere, carbon will diffuse to the surface and there be "burned" away. After a sufficient

⁶Studies of the three-dimensional form of graphite in cast iron include: Roll 1928; Merchant 1961; Kusakawa & Nakata 1963; Li Chunli et al. 1983; Murthy et al. 1986.

time the carbon content of the casting is reduced to a sufficiently low level that the iron is fairly strong and tough.

During the anneal another process may also operate: cementite may decompose to form graphite ($\text{Fe}_3\text{C} \rightarrow 3\text{Fe} + \text{C}$). Graphite precipitated in iron in the solid state is in the form of microscopic nodules which are much more rounded than the flakes precipitated in the solidification of grey iron, and the graphite therefore has much less effect on the mechanical properties of the iron.

Malleable cast iron is termed *whiteheart* if the most important effect of the anneal is decarburization, and *blackheart* if the most important effect is graphitization. (Again the terms come from the usual appearance of the fracture in older practice; see e.g. the illustrations in Gilbert 1954 and Moore 1960.) Whether decarburization takes place depends on whether the annealing atmosphere is oxidizing or neutral. Whether graphitization takes place depends on the annealing time and temperature, but especially on the chemical content of the iron. For example silicon favours graphitization and sulphur retards it. Cast iron is never (never) a simple alloy of iron and carbon. Significant amounts of silicon, sulphur, manganese, and phosphorous are always present. Other alloying elements will usually also be present, either intentionally or unintentionally. All of these alloying elements influence the nucleation and growth of graphite, often in surprising ways.

3. The simplest case: decarburization without graphitization

Figure 6 shows a fragment of a hoe-head from the ancient copper-mine site at Tonglushan in Daye, Hubei 湖北大冶铜绿山. Its chemical analysis is given in Table I, no. 2. It is 3 mm thick. Metallographic examination (Ye Jun 1975) indicates that it is composed of five layers (see figure 7):

ferrite (ca. 0 carbon)	1.0 mm
pearlite (ca. 0.8% C)	0.2 mm
ledeburite (ca. 4.3% C)	0.6 mm
pearlite	0.2 mm
ferrite	1.0 mm

The ferrite grains are columnar, growing inward from the surface. The boundaries between layers are well-defined.

This is a remarkably tough structure: the metallurgists who did the examination were able to bend the artifact to an angle of 90° with

no sign of breaking except some surface cracks.⁷ This would not have been possible with either white or grey cast iron.

A metallurgist with some experience with such things will see immediately that one way of producing this structure is to cast the hoe-head in white cast-iron, then anneal it in an oxidizing atmosphere for a period of days in the temperature range in which ferrite and austenite can exist together in equilibrium, 723–910°C. It turns out that an even more precise description of the proposed anneal is possible. By my calculation the temperature should be about 750°C and the annealing time about 12 days.

The thicknesses of the ferrite and pearlite layers, p_α and p_γ are given by

$$p_\alpha = K_\alpha \sqrt{t}$$

$$p_\gamma = K_\gamma \sqrt{t}$$

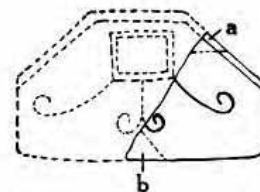
where t is the annealing time in days, p_α and p_γ are in mm, and K_α and K_γ depend only on the annealing temperature and the initial carbon content of the white iron casting. Calculated values of K_α , K_γ and K_γ/K_α are given in Table V and plotted in figure 8. (The derivation of the formulas and the method of calculating K_α and K_γ are given in section 7 below.) In the present case $p_\alpha = 1.0$ mm, $p_\gamma = 0.2$ mm, and therefore $K_\gamma/K_\alpha = 0.2$. Consulting figure 8, the annealing temperature which corresponds to this value of K_γ/K_α is very close to 750°C. At this temperature $K_\gamma = 0.057$ mm/day^{1/2}. Then

$$t = \left(\frac{p_\gamma}{K_\gamma} \right)^2 = \left(\frac{0.2}{0.057} \right)^2 = 12 \text{ days.}$$

This is a surprisingly long annealing time. At a higher temperature an equally good or better structure could have been obtained in a much shorter time. However if the test used for satisfactory completion of the anneal was a soft surface which for example could be filed easily, then a lower temperature would have been chosen, since this gives the fastest growth of the soft ferrite layer.

The above discussion gives *one* way in which the structure found in the hoe-head fragment could have been produced, but this is not the only way. The temperature would have varied considerably over this

⁷This sort of test of the gross physical properties of an ancient artifact is not usually possible, because of the effects of corrosion; but the ancient mine shafts at Tonglūshan have provided an oxygen-free environment in which the iron implements have been beautifully preserved with hardly a trace of corrosion.



图一三 六角铁锄残片取样部位

Figure 6 Hoe-head fragment from the ancient copper-mine site at Tonglūshan (Ye Jun 1975: 25).



Figure 7 Micrograph from the hoe-head fragment shown in figure 6. (Li Zhong 1975, plate 1.5). Etched with nital.

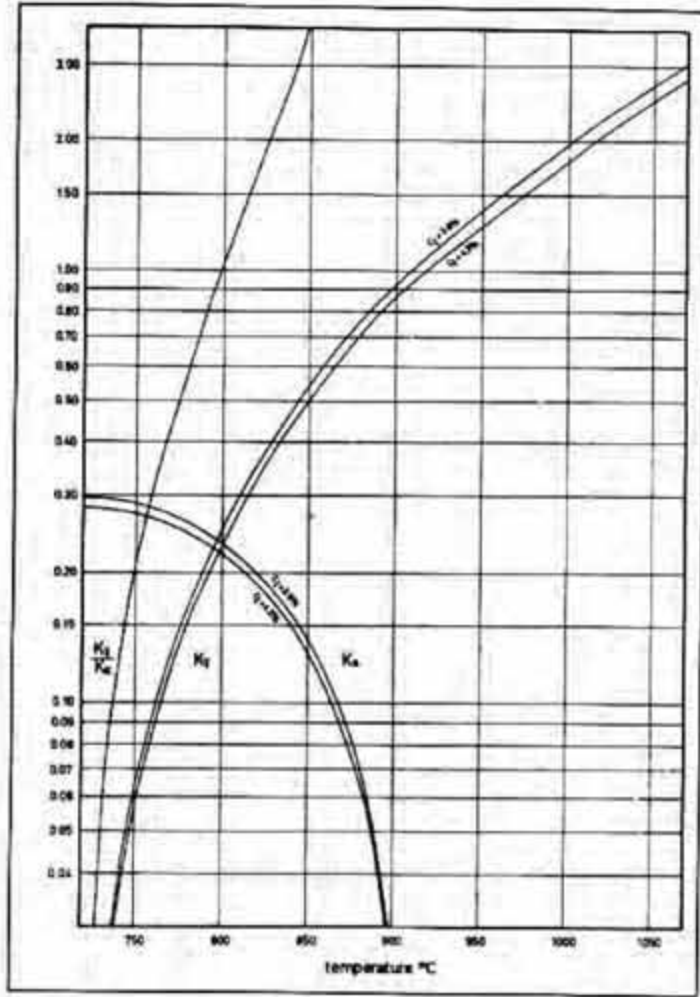
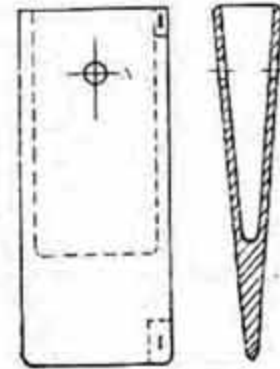


Figure 8 Calculated values of K_x , K_y and K_x/K_y plotted against annealing temperature T for two values of the initial carbon content C_1 . The dimensions of K_x and K_y are $\text{mm/day}^{1/2}$. When $T \geq 910^\circ\text{C}$, $K_x = 0$. Values of K_x/K_y for different C_1 are so close that they are represented by a single line.



图五 巩县铁钎（临6）
I、II，试样部位，A，器壁的
铸出孔（固定木叶用）

Figure 9 A cast-iron mattock-head found in 1959 at the site of a Han-period ironworks at Tieshenggou in Gongxian County, Henan. Artifact no. lin 临-5 (Hua Jueming et al. 1980: 3).



Figure 10 Micrograph from the mattock-head shown in figure 9. Unetched, crossed nicols. This micrograph was kindly supplied by Dr. Guan Hongye of the Foshan SG-iron Research Institute in Foshan, Guangdong.

long annealing period, and at the least the statement "twelve days at 750°C" must be modified to "on the order of twelve days at a rather low temperature". Furthermore a somewhat similar structure can be obtained by decarburizing first at a much higher temperature for a shorter time, then cooling very slowly; see for example Gilbert 1954, figures 4, 6, 8, and 10. Further theoretical and experimental work may make it possible to distinguish the structures obtained in these two ways.

The derivation of the equations given above is rather complex, and involves some simplifying assumptions; therefore I will not be satisfied that the result is correct until I have had a chance to test it empirically. Furthermore the corresponding calculations for the decarburization of a *cylindrical* object, for example a collection of white-heart malleable cast iron arrowheads studied by Du Fuyun (1981), involve much less tractable differential equations than those for a flat plate. Here we may well prefer to rely on empirical data rather than theoretical calculations. Nevertheless the point to be made here is that the physical laws which govern diffusion of carbon in iron are well known, because they have been the subject of much study in the past century or more. Even if we choose to rely on empirical rather than theoretical methods, we know with considerable certainty which factors affect the process and which do not, and the results will be rather certain.

4. Blackheart malleable cast iron

Where graphite precipitation is involved the situation is much more difficult. The physical laws which govern graphite nucleation and growth are very poorly understood, and therefore the annealing parameters cannot be determined by a simple calculation. Instead we must rely on trial-and-error empirical studies: for a given artifact a set of samples is cast with the same chemical analysis, and these are annealed at various temperatures for various times until the microstructure seen in the artifact has been obtained in one of the annealed samples. This is obviously an extremely time-consuming and expensive process, but there is a more fundamental difficulty. We are not even sure that we know all of the parameters which influence graphitization, so we cannot be sure that an experimental study of the kind outlined here has taken account of all relevant parameters.

Modern foundry literature gives a great deal of empirical data on the effects of various factors on the microstructure of malleable cast iron, though the application orientation of most of it must be con-



Figure 11 Micrograph from a hoe-head excavated at the late Warring States period city-site Yanxiadu, in Yixian County, Hebei (Li Zhong 1975, plate 1.4).

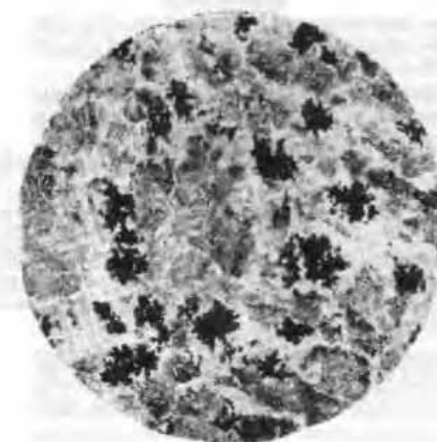


Figure 12 Micrograph from a mattock-head excavated at a Han-period iron-works site at Wafangzhuang in Nanyang, Henan (Hua Jueming 1982, plate 2.4a). Etched with nital.

stantly borne in mind. A good survey of the literature is Wieser 1967, and it is the basic source for the following discussion.

The graphite precipitates as microscopic nodules with shapes that may be classified as follows:

1. Spherulites. These are distinguished from the next by a radiating structure which can be seen especially with crossed nicols. An example is shown in figure 10.
2. Compact aggregates, as in figure 11.
3. More or less "sprawly" aggregates, or "nests", as in figure 12.

Other factors being equal, the mechanical properties of the resulting iron are best with spherulitic graphite, lower with compact aggregates, and lower again with sprawly aggregates. In any case they are better than those of grey cast iron, and of course much better than those of white cast iron, for most ordinary applications.

Graphitization of white cast iron can be considered to consist of two consecutive processes: *nucleation* and *growth*. Each nodule grows from a nucleus. The number of nuclei (e.g. per mm³) influences directly the time for full graphitization, since each nodule grows at a rate determined by other factors.

It was formerly believed that the type of nucleus determines the shape of the nodule; in particular that spherulitic graphite grows from FeS inclusions in the iron, while other forms grow from other (unidentified) types of inclusions. It was shown long ago that this is not the case.

It has been observed that *some* temper graphite spherulites contain FeS inclusions at the centre (e.g. Morrogh 1941: 220). Some authors have claimed that *all* graphite spherulites have FeS nuclei (e.g. Loper & Takizawa 1965). However it was shown many years ago that the supposed FeS nuclei found by these authors are what we might call an "optical illusion":

When a graphite spherulite is sectioned away from the centre, the central zone of the section consists of graphite crystallites cut parallel to the basal plane giving specular metallic reflection. This was explained by Morrogh and Williams⁸ who pointed out that this bright spot should not be mistaken for a nucleus; nevertheless a vast literature developed on the nature of this spot and many wild theories were proposed for the composition of this nucleus. However, it seems that the true nature of this basal graphite surface is now fairly generally recognized.

(Morrogh 1955: 662)

⁸In *Journal of the Iron and Steel Institute*, 1947, 155: 321-371.

A pseudo-nucleus of this type can be seen in figure 23, lower left; in this iron, before annealing, no FeS inclusions were seen, and indeed none would be expected in iron of this composition (0.03% Mn, 0.014% S). Loper and Takizawa (1965: 526-527) claim to have found an FeS nucleus in every spherulite examined; with the experimental method described, if their theory had been correct, they should have found FeS nuclei in only about half of the spherulites examined.

It is more likely that the nuclei on which temper carbon grows are submicroscopic discontinuities, only a few atoms in size, in the crystal structure of the iron. A plausible hypothesis is that such discontinuities are more likely to occur at or near phase boundaries; this would account for the fact that graphite nodules often appear to have grown from inclusions of FeS or MnS. The exact nature of the graphite nuclei remains a submicroscopic mystery, but in any case it now seems to be certain that the shape of the nodules is independent of the type of nucleus, and is determined only by growth conditions. It is a peculiar and misleading fact that graphite precipitated in white cast iron in which FeS inclusions are present is almost always spherulitic. Apparently the presence of FeS inclusions is normally accompanied by other conditions in the iron which favour the growth of spherulitic graphite.

Growth conditions determine both the shape of the graphite nodules and the rate of their growth. The graphite crystal is hexagonal, with two possible growth axes called *a* and *c*. A very important empirical fact is that flake graphite (as in grey cast iron) grows in the *a* direction, spherulitic graphite grows in the *c* direction, and aggregates grow in both directions simultaneously. Whether an aggregate grows to be compact or sprawly depends on the relative growth rates in the two directions. Many parameters influence the growth rate; some of these are discussed below. In general these can be expected to affect *a*- and *c*-axis growth differently, so that graphite shape is also affected.⁹

4.1. Foundry practice. Nucleation of graphite is affected by melting and casting procedures. Oxidizing conditions in the melting furnace decrease nucleation. A high solidification rate in the mould is said to

⁹The theory of graphite morphology described in this paragraph seems to be very widely accepted by metallurgists, but in fact considerable doubt has been thrown on it by the experimental results of Hunter & Chadwick (1972a; 1972b) and of Johnson et al. (1974). Note also Ohide & Ohira 1970. It may be that it will be necessary, before clarity on this matter can be achieved, to study the mathematics of diffusion-limited aggregation and fractal growth; for a popular introduction to this deep and difficult new branch of mathematics see Sander 1987.

increase nucleation;¹⁰ but note the experimental results reported in section 5 below. The melting temperature and the time held at temperature before pouring probably also have some effect (Schneidewind & White 1933).

Something is known of ancient Chinese foundry practice, though not nearly as much as we should like. A great many cast-iron moulds for cast-iron implements have been found (e.g. figure 13),¹¹ and there is a striking correspondence between the types of implements which have been found to be of malleable cast iron and those for which cast iron moulds have been found. It seems likely, therefore, that all or most malleable cast-iron implements were cast in cast-iron moulds. This and the fact that these implements are very thin (2-3 mm) imply that solidification was very rapid. In addition the use of cast-iron moulds implies that the melting temperature must have been very high. It is very likely that the iron was melted in a cupola furnace; not only because this is the simplest way of melting iron, but also because an ancient cupola furnace has in fact been excavated (KGXB 1978.1: 11-13). The atmosphere near the bottom of a cupola furnace would be expected to be oxidizing.

The ancient Chinese use of cast-iron moulds was probably motivated by a straightforward economic consideration: mass production of agricultural implements was easier and cheaper with permanent moulds. It may also be, however, that it was learned that rapid solidification decreases the required annealing time, because of increased graphite nucleation.

4.2. Special pre-annealing treatments. A wide variety of rather peculiar treatments of the casting before annealing have been reported to increase graphite nucleation. These include heating to 950°C and cooling in air (Engel 1944: 86-87); heating to a similar temperature and quenching in water;¹² ultrasonic vibration; and permanent cold-deformation of the casting. (It is amazing that this last should be contemplated for white iron castings.) None of these treatments has been studied in enough detail to allow an explanation of how they work, but it seems possible that they are all somehow related to the creation

¹⁰Kikuta 1926: 129-131; Boegehold 1938: 480-481; Schneidewind et al. 1947.

¹¹On ancient Chinese cast-iron moulds for casting iron implements see FTJ 1973 (in English); Zheng Shaozong 1956; Zi Xi 1957; Li Buqing 1960; Yang Gen & Ling Yeqin 1962; Li Jinghua 1965; Zhang Zigao & Yang Gen 1973; Zhu Huo & Bi Baoqi 1977. Note that ceramic moulds have also been found for a few of the same implement types; see e. g. Chen Yingqi & Li Enja 1986: 118-120.

¹²Schneidewind & Reese 1949: 505; M. Tilley in Schneidewind 1950: 207; Tkachenko & Maistruk 1962.



Figure 13 Two-piece cast-iron mould for casting an iron hoe-head like that shown in figure 6. This was found at a Warring States period site in Xinglong, Hebei (Guo Moruo 1973, plate 7).

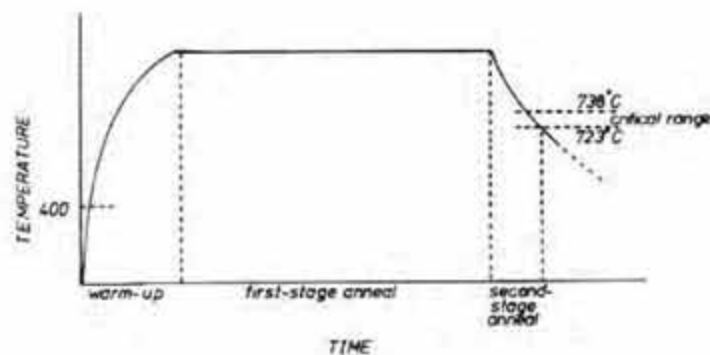


Figure 14 Typical temperature cycle in modern annealing of blackheart malleable cast iron.

of microscopic internal cracks in the iron. Other even more exotic pre-anneal treatments include passing an electric current through the casting, subjecting it to an alternating magnetic field, and irradiating it with gamma rays.

4.3. Annealing temperature cycle. The annealing cycle may in general be supposed to be as shown in figure 14. In modern industrial practice the annealing temperature T is generally in the vicinity of 950°C. The warm-up time may be as long as 24 hours, because many tons of castings are annealed together. The first-stage anneal is on the order of 2–4 days, and the second stage on the order of 1 day.

The warm-up time is known to have a marked influence on the number of graphite nuclei.¹³ Studies have shown that the important factor is the time spent in a relatively narrow temperature range somewhere in the vicinity of 400°C, and that this influence is heavily dependent on the ratio of manganese content to sulphur content. At Mn/S = ca. 3, several hours at 350°C can quintuple the number of nuclei, while the effect is negligible at Mn/S < 1 and decreases as Mn/S increases over 3. These effects have not been investigated at the low levels of manganese and sulphur typical of ancient Chinese cast iron.

During the first-stage anneal cementite breaks down to form austenite and graphite ($\text{Fe}_3\text{C} \rightarrow 3\text{Fe} + \text{C}$). The graphite grows on the nuclei which are present; if there are no nuclei, the cementite does not break down. Each graphite nodule grows at a rate which is dependent on the temperature and on the chemical content of the iron in its immediate microscopic vicinity, which need not be the same as the gross chemical analysis of the iron.

The temperature of the first-stage anneal affects the shape of the graphite nodules. Aggregates are more sprawly with high temperatures, more compact with lower temperatures; thus it would seem that a -axis graphite growth is more dependent on temperature than c -axis growth. In modern practice the annealing temperature chosen is a compromise between cost and quality: at higher temperatures the required annealing time is shorter, and at lower temperatures the graphite shape is superior (see e.g. Schwartz 1922: 214).

During the second-stage anneal, as the temperature falls the maximum carbon content of the austenite decreases, and the excess carbon precipitates as graphite on the graphite nodules produced in the first-stage anneal. When the temperature reaches 738°C, the eutectoid temperature in the stable iron-graphite system, the austenite

¹³See e.g. Boegehold 1938: 480–481; Schneidewind & Reese 1949; Schneidewind 1950: 204; Gamol'skaya & Rabinovich 1964; Todorov & Nikolov 1970; Tsutsumi & Hoshibara 1975.

has a minimum carbon content of 0.69%. In the "critical range", 738–723°C, austenite transforms to ferrite + graphite. At 723°C any remaining austenite transforms to ferrite + pearlite according to the metastable iron-cementite system, and below this temperature there is very little likelihood of graphite growth.¹⁴

In the second-stage anneal the most important factor is the cooling rate. If the cooling is sufficiently slow, especially in the critical temperature range, the result is graphite in a ferrite matrix. With faster cooling rates the matrix also contains pearlite; this gives a product which is harder, which is desirable in many applications, but the tensile strength is not necessarily improved, since this is limited by the presence of the graphite nodules.

Most ancient Chinese blackheart malleable iron artifacts contain some pearlite in the matrix. This may imply that the second-stage cooling rate was rather fast, but it may also be that at low silicon levels an extremely slow cooling rate is required for complete graphitization.

4.4. Chemical composition. Within the ranges encountered in modern practice, the following effects are well established.

Carbon: Increased carbon content increases nucleation. However it can increase the total time required for first-stage graphitization, since with a higher carbon content there is more cementite to be broken down.

Silicon: Nucleation increases with increased silicon content. In one study (using iron with 2.3% C, 0.5% Mn, and 0.05% S) a silicon content of 1.9% gave 1½ times as many graphite nodules per volume as 1.1% (Wieser 1967: 48).

Sulphur and manganese:¹⁵ The actual content of these elements is considered to be less important than their ratio. When Mn/S = 1.7, nearly all of both elements is in the form of MnS inclusions. A slightly higher ratio, sometimes stated to be Mn = 1.7S + 0.15%, gives a dramatic increase in nucleation. (But see section 4.3 above.) Still higher ratios decrease nucleation. At ratios Mn/S < 0.7 a -axis graphite growth appears to be suppressed. This means that total graphite growth is very slow, but that the resultant graphite is nearly spherulitic.

¹⁴In modern practice this description of the second-stage anneal is complicated by the high silicon content of the iron. With high silicon content there is a temperature range in which austenite, ferrite, and graphite can exist together in equilibrium, and this presumably influences the rate of second-stage graphitization.

¹⁵Hultgren & Östberg 1954; 1955; Rote et al. 1956; Stein et al. 1970.

It is often assumed that the only way of producing spherulitic graphite by annealing is to use $Mn/S < 0.7$; however an axe-head from the Mianchi scrap-heap (no. 18 in Table I) contains spherulitic graphite, but has $Mn/S = 2.5$. Clearly other factors are also involved. See also the experimental results reported in section 5 below.

Boron: Addition of very small amounts of boron can increase graphite nucleation dramatically (see e.g. Fominykh et al. 1967). In one study the optimum addition was 0.003%; this increased nucleation fourfold. Smaller and larger additions gave smaller increases. The boron is usually added by mixing borax ($Na_2B_4O_7 \cdot 10H_2O$) into the molten iron before casting; only a small part of the boron in the borax is reduced and enters the iron, but borax is cheap, and only a very small quantity of boron is required in the iron.

The use of borax as a soldering flux appears to have been known in China as early as the Song period (Wang Jiayin 1957: 54), and China has long been famous for its borax production (see e.g. Grill 1772; Geerts 1883: 319-321). I do not know whether borax was known in China as early as the Han or before, but if it was it might easily have been tried as an addition to molten iron and been found to decrease the necessary annealing time. No analyses have been published for boron in ancient Chinese artifacts, and indeed it is difficult to see how the small quantities involved could be detected without sacrificing a very large sample of the artifact in the analysis.

Other alloying elements: Various other alloying elements have been shown to influence graphite nucleation and growth. Some of these are discussed by Kikuta (1926: 132-145), Wieser (1967) and by Angus (1976). In general it must be presumed that every single alloying element present in the iron will have some effect. Some may turn out, as in the case of boron, to have significant effects at almost undetectable levels.

This survey of the factors influencing graphite nucleation and growth has been based on published experimental studies. Most of these studies are narrowly oriented to the improvement of modern malleable foundry practice, and are therefore of limited usefulness in a study of ancient Chinese malleable cast iron artifacts. Replies to a questionnaire from 32 malleable foundries in the United States (Hernandez 1967: 606, 610) indicated that the chemical composition of melting stock was normally within the following limits:

C	2.5 - 2.8%
Si	1.15 - 1.6%
Mn	0.3 - 0.5%
S	0.06 - 0.13%
P	0.02 - 0.12%

Comparison with Table I shows that the ancient Chinese cast iron artifacts have, in comparison with modern malleable cast iron, high carbon and phosphorous, low manganese and sulphur, and extremely low silicon content.¹⁶ The difference in silicon content may be the most important factor here. Very few of the published studies which I have consulted in the above survey consider alloys with less than 1% Si, and none at all considers alloys with less than 0.5% Si. But the silicon content of the ancient Chinese cast iron artifacts is usually under 0.2%.

Some attempts have been made to summarize the available empirical studies in quantitative terms; an example is that of Schneidewind (1950). The suggestion has been made to me that we have here the only key necessary to an understanding of ancient Chinese malleable cast iron. However the apparent precision of the formulas given by Schneidewind is fictive, as he himself is at pains to make clear.¹⁷ In their derivation the simplifying assumption is explicitly made that the influence of each factor is independent of the other factors, and this is known to be untrue. For example the carbon content of the iron influences the degree to which the silicon content influences graphite growth rate (Rehder 1949; Schneidewind 1950: 206). Furthermore application of Schneidewind's formulas to the ancient Chinese artifacts would involve an implicit extrapolation far outside the limits of the empirical data on which the formulas are based.

5. Experimental results

It should be clear from section 4 above that the modern experimental work which has been done on blackheart malleable cast iron gives some useful indications of the ways in which various parameters influence graphitization, but that none of its results can be applied directly to the ancient Chinese artifacts, because of differences in chemical content and foundry practice. It is therefore clear that new experi-

¹⁶Thus the experiments reported by Rostoker (1988), in which he anneals an iron with 0.78% Si and 0.27% S, are irrelevant in the study of ancient Chinese malleable cast iron artifacts.

¹⁷"It may safely be said that in view of the variables mentioned and the many possible ones not recognized, no computations can be made at the present time from which on a theoretical basis the annealing rate can be predicted. This paper will attempt to summarize the quantitative knowledge of those variables which are fairly well understood and to list some of the problems yet to be solved before a complete understanding of graphitization can be achieved" (Schneidewind 1950: 202). Note also the more blunt, not to say angry, criticism of a practical foundryman, Milton Tilley, in Rehder 1949: 180.

mental work, directed toward the specific characteristics of ancient Chinese malleable cast iron, is necessary.

I have started a series of experiments along this line. Some results are reported below, and some of these are rather surprising. A great deal more work is needed; I intend to continue, but I hope that others will also become interested in this sort of work.

The iron used was a very unusual white cast iron supplied by the Department of Mechanical Technology of the Technical University of Denmark, with the following analysis:

C	Si	Mn	P	S
3.80	<0.01	<0.03	0.015	0.014

Ni	V	Cu	Ti	Al	Cr	Mo	Sn	Mg
0.080	0.03	0.026	0.000	0.00	0.0	0.0	0.0	0.00

The first five items above are from a wet chemical analysis done at Varde Steelworks, Varde, Denmark; the rest are from a Quantovac analysis done at Korrosionscentralen, Copenhagen.

This iron was melted in open ceramic-graphite crucibles in a medium-frequency induction furnace. The melt was poured white-hot, but its temperature was not measured. Charges of 2 kg were melted, and ferrosilicon with 70% Si was added to the melt to adjust the silicon content: 3 g ferrosilicon for 0.1% Si (series 500 and 800), 6 g for 0.2% (series 600 and 900). The actual resulting percentages, determined by Quantovac analysis, are shown in the tables.¹⁸ It will be noticed that the actual Si content of series 500 is much lower than intended.

In the experiments reported in Tables II-III the iron was cast in bars 400 mm long with a triangular cross-section, ca. 30 mm x ca. 45 mm. An open mould of welded 8 mm steel plate was used; this is the smaller of the two shown in figure 15. These bars were cut into wedges with length 20-30 mm. Samples 401-414, 501-514, and 601-614 were cut from bars 4, 5, and 6 respectively.

In all cases the annealing was done in annealing pots made of 18/8 stainless steel pipe, inside diameter 50 mm, length 240 mm, with a cap welded on one end. Samples were packed in grey cast-iron turnings. The pots were closed with tight-fitting stainless steel disks and luted with 20-30 mm refractory cement. In two cases (Table IV) parts

¹⁸The laboratories warn that it is extremely difficult to analyze for Mn and Si at such low levels, and that the results may not be as exact as they appear in the tables.

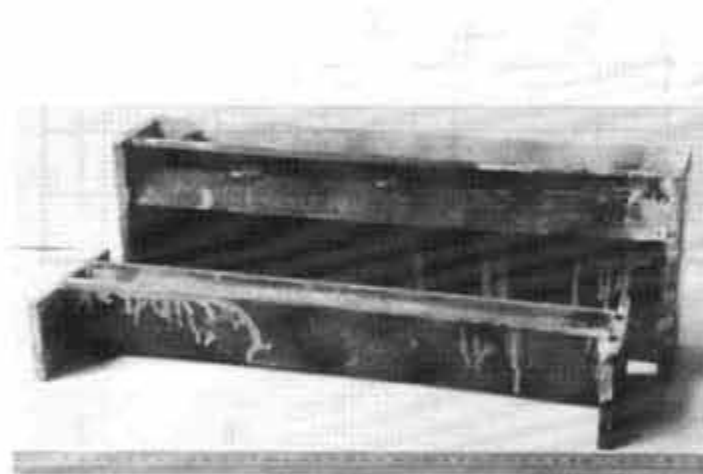


Figure 15 Moulds used to cast samples for the annealing experiments.

Table II Annealing of white cast-iron wedges as described in the text, section 5. After pre-treatment at 950°C, if any, all samples were held at 400°C for 20 hours; then transferred to a pre-heated 950°C oven and held for 144 hours (6 days); then transferred to a pre-heated 750°C oven for 23 hours; then cooled in air.

sample no.	Si %	as cast	pre-treatment 950°C		graphite nodules / mm ²	diameter of largest nodule, μm	notes
			quenched in water	cooled in air			
401	0.02	✓			0	—	
402	*		✓		0.35	200	one nodule found
403	*			✓	ca. 0	(100)	
501	0.03	✓			0.38	200	
502	*		✓		0.57	100	
503	*			✓	1.3	300	
601	0.22	✓			7.4	100	
602	*		✓		4.8	200	
603	*			✓	4.6	300	

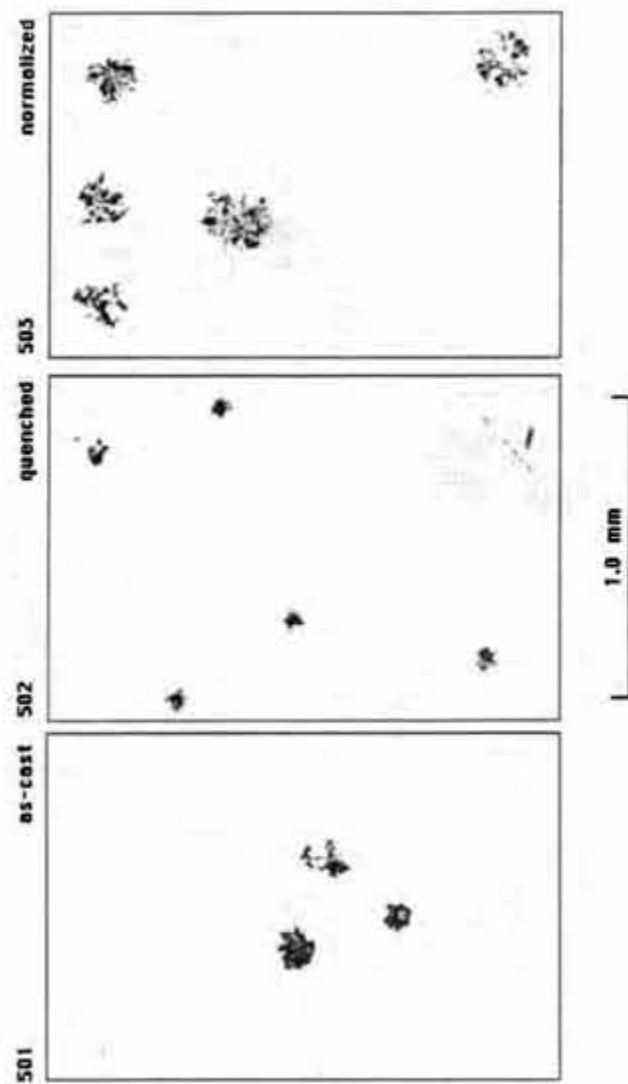


Figure 16 Graphite in samples 501, 502, and 503; see Table II. Unetched.

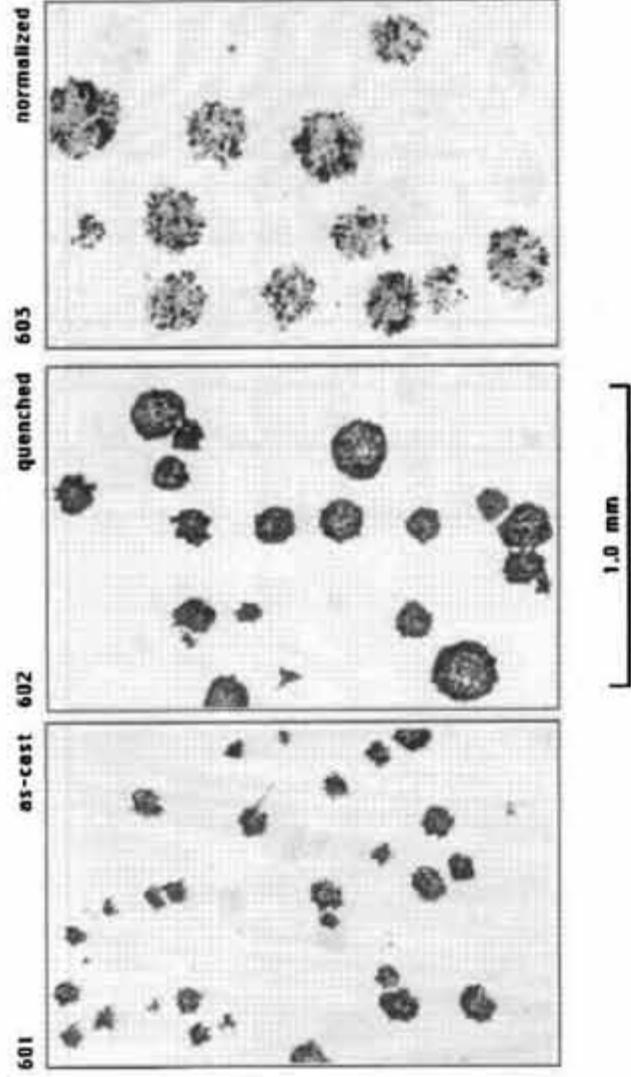


Figure 17 Graphite in samples 601, 602, and 603; see Table II. Unetched.

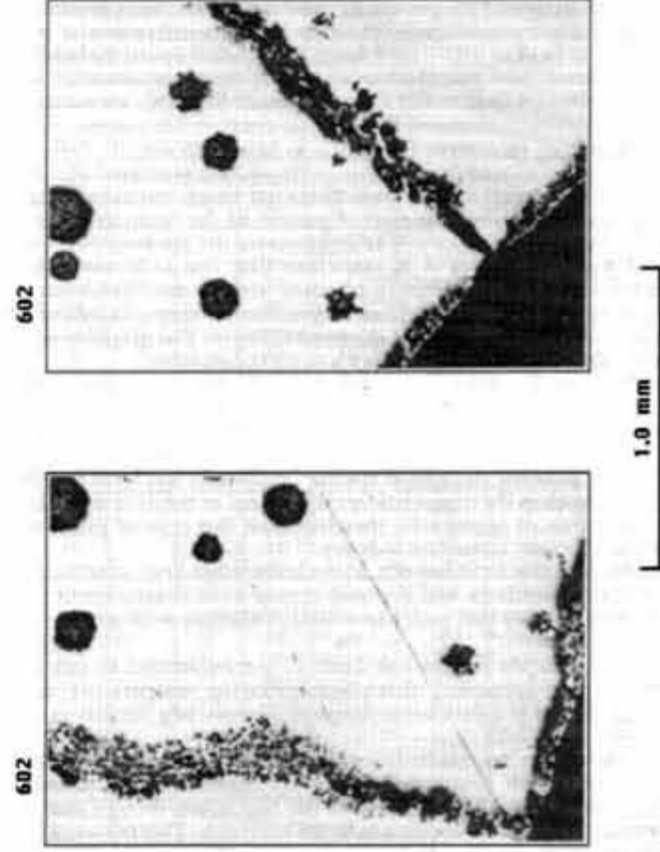


Figure 18 "Snakes" of graphite in sample 602; see Table II. Unetched.

of samples were slightly surface-decarburized; this indicates that in these cases the annealing pots were not adequately sealed.

The intention of the first series of experiments (Table II) was to test the effect of two of the pre-anneal treatments discussed in section 4.2 above. Samples were annealed either as-cast or after one of two treatments: (1) held at 950°C for $\frac{1}{2}$ hour, then cooled in air; (2) held at 950°C for $\frac{1}{2}$ hour, then quenched in water. All were then annealed for 20 hours at 400°C, 6 days at 950°C, and 23 hours at 750°C, then cooled in air.

The resulting structures are shown in figures 16 and 17. Table II gives the number of nodules per mm² in the section examined and the diameter of the largest nodule seen. These are rough measures of the extent of nucleation and the rate of growth of the nodules respectively. The results seem to show an influence of the pre-treatments on graphite nucleation, but it is not clear that the differences are significant when the difficulties of counting nodules are considered. If the differences noted are significant they indicate a very odd influence of Si content on the influence of the pre-treatment. The graphite nodules were all compact aggregates with some polarization.

In the samples which were quenched in water before annealing, graphite was found not only in nodules but also in long "snakes" which appeared to follow microscopic cracks in the iron; see figure 18. This could be explained by hypothesizing that graphite nuclei form very densely at or near the surfaces of cracks. Graphite in this form may be expected to weaken the iron considerably, almost as much as the flakes in grey cast iron. It seems odd, therefore, that this type of pre-treatment should be used in modern industry.

Graphite in this form has not, to my knowledge, been observed in ancient Chinese artifacts, and it would appear to be reasonable to disregard the possibility that such pre-anneal treatments were used.

The experiments reported in Table III were intended to test the effects of warm-up period, first-stage annealing temperature, and silicon content on graphitization. Some of the resulting structures are shown in figures 19-21.

It is clear from the results that slow warm-up time and increased silicon content both encourage nucleation considerably. Increased first-stage annealing temperature also has this effect, though sample 607, annealed at 1000°C, appears to be an exception. This is one of the samples in which complete first-stage graphitization was reached, and one possibility is that in a late stage of the anneal larger nodules grew by diffusion of carbon from smaller ones, so that some nodules entirely

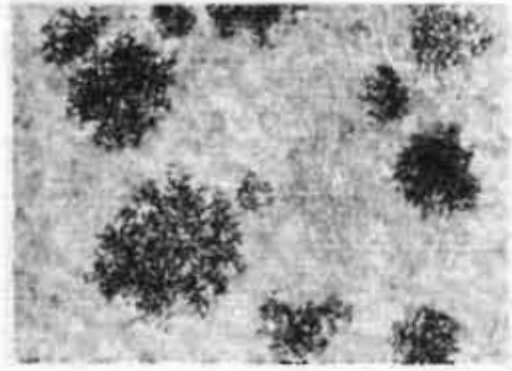
Table III Annealing of white cast iron wedges as described in the text, section 5. Half the samples were held at 400°C for 20 hours; then all the samples were transferred to ovens pre-heated to the temperatures indicated. After 144 hours (6 days) the samples were removed from the furnaces and cooled in air.

All graphite was found to be in the form of compact aggregates.

In most samples a heavily graphitized skin was found. Its thickness is indicated in the seventh column.

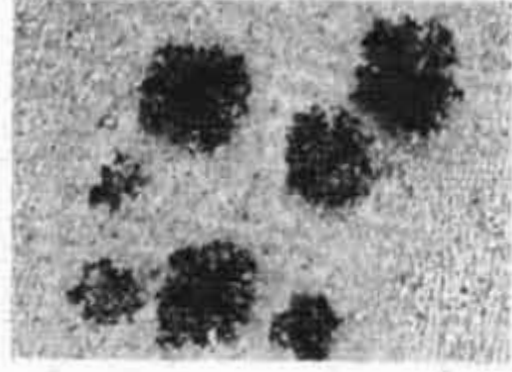
In most samples massive cementite remained from the original ledeburite. However in samples 607, 608, 609, and 611 the original cementite was completely decomposed, and the matrix was pearlite + proeutectoid cementite.

Sample no.	Si %	20 hrs at 400°C	144 hrs at °C	graphite nodules / mm ²	diameter of largest nodule, μ m	thickness of graphitized skin, μ m	notes
407	0.02	✓	1000	ca. 0	100	50	24 nodules observed
408	"	✓	950	ca. 0	(300)	40	3 nodules observed
409	"	✓	900	ca. 0	(300)	40	1 nodule observed
410	"	✓	850	0	—	10	
411	"		1000	ca. 0	300	50	12 nodules observed
412	"		950	0	—	30	
413	"		900	ca. 0	(300)	20	2 nodules observed
414	"		850	0	—	10	
507	0.03	✓	1000	1.1	450	50	
508	"	✓	950	1.5	300	30	
509	"	✓	900	0.8	300	80	
510	"	✓	850	0	—	10	
511	"		1000	1.6	450	50	
512	"		950	ca. 0	150	20	15 nodules observed
513	"		900	ca. 0	(300)	80	5 nodules observed
514	"		850	0	—	10	
607	0.22	✓	1000	13	100	50	complete first-stage graphitization
608	"	✓	950	28	90	100	"
609	"	✓	900	19	300	40	"
610	"	✓	850	6.7	50	20	
611	"		1000	7.1	200	50	complete first-stage graphitization
612	"		950	1.5	300	100	
613	"		900	1.8	300	80	
614	"		850	1.2	50	20	



507

0.03%
SI



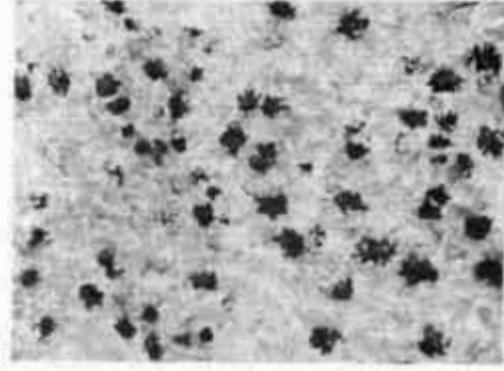
511

1.0 mm

slow wormup

fast wormup

607

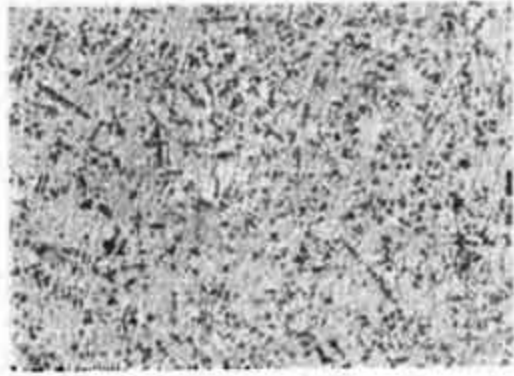


0.2%
SI

611

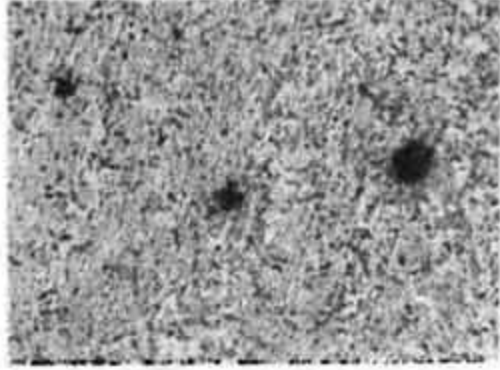


Figure 19 (both pages) Micrographs from samples 507, 511, 607, and 611; see Table III. Etched with nitric.



510

850°C



509

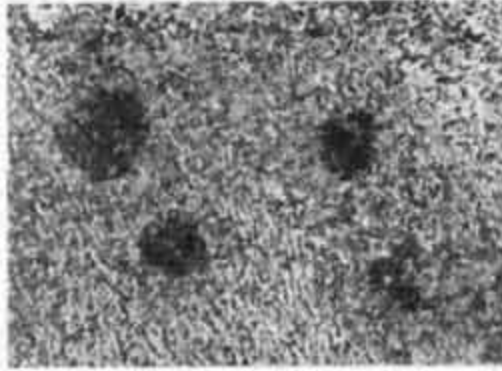
900°C

1.0 mm

Figure 20 (both pages). Micrographs from samples 510, 509, 508, and 507; see Table III. Etched with nitric.

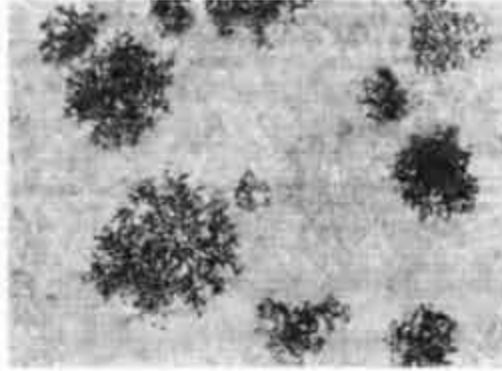
508

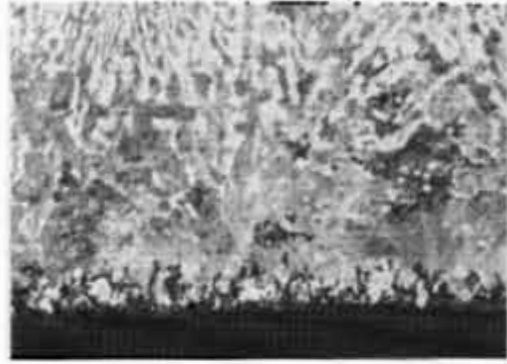
950°C



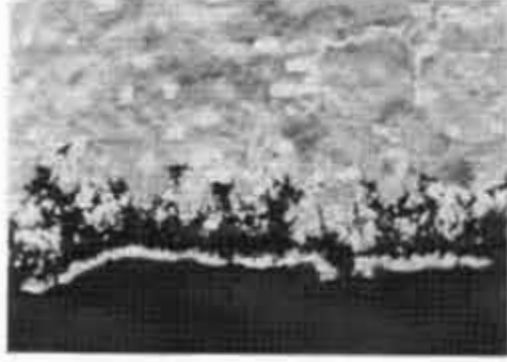
507

1000°C





409



507

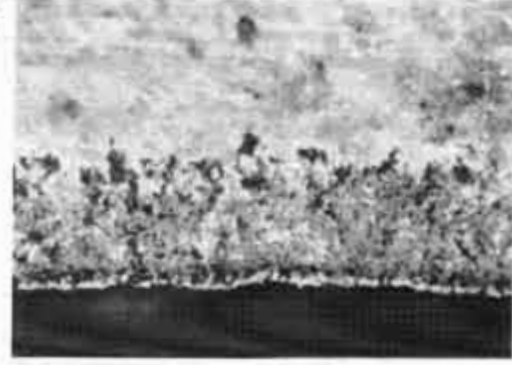
0.2 mm

Figure 21 (both pages) Micrographs showing the heavily graphitized skin in samples 409, 507, 609, and 612; see Table III. Etched with nitric.

609



612



disappeared as annealing proceeded far beyond the time necessary for first-stage graphitization.

Complete first-stage graphitization was achieved only in samples with the highest silicon content. Thus first-stage annealing time for these samples was less than 6 days, and would be considerably longer for the others.

In each sample a heavily graphitized "skin" was observed at the surface. Four examples are shown in figure 21. The thickness of each skin is given in the table. This skin was sometimes as much as 90% graphite by volume, and the iron directly under it was sometimes 100% pearlite with no cementite remaining from the original ledeburite.

This same phenomenon has been observed in white cast iron samples annealed in dry hydrogen, argon, or a vacuum (Bernstein 1948, figs. 3-5; Dawson & Smith 1956: 227). In the present experiments the samples were packed in grey cast iron turnings during the anneal, so that the atmosphere in the annealing pots should be expected to have been composed largely of nitrogen and carbon monoxide. Dr. H. Morrogh writes: "Broadly speaking, we believe we know now that free energy and surface energy considerations cause graphite at high temperatures to migrate to cover all surfaces. The form of the deposition on the surface depends on those factors influencing the crystal growth habit of the graphite" (personal communication, 2nd October 1984). It seems likely, then, that this graphite skin is always formed during the anneal, but that if the atmosphere is more than very slightly oxidizing the graphite is immediately burned away. However the fact that such a skin is not more widely noticed in the foundry literature suggests that there may also be some more complex factors involved, e.g. in this case the very low silicon content and the high solidification rate in the iron mould.

It seems likely that the same phenomenon would also have occurred in the annealing of some ancient Chinese castings. The graphitized skin would very quickly have been lost, either in post-anneal cleaning or in the use of the implement. It is therefore possible that the decarburized layer seen in most ancient Chinese blackheart malleable artifacts is in some cases caused by graphite growth in the skin rather than by an oxidizing atmosphere.

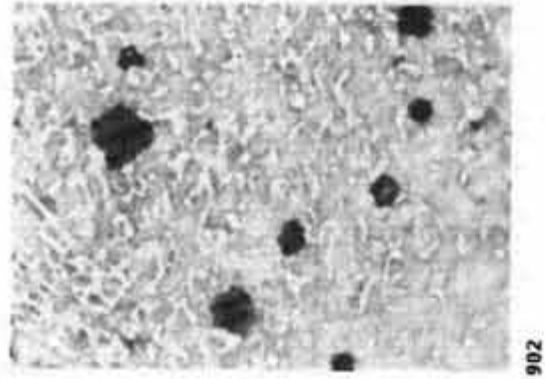
In the experiments reported in Table IV the iron was cast as a plate, intended to be 400 × 100 × 3 mm. The mould used is the larger of the two shown in figure 15; it is made of 8 mm welded steel plate, with a very large casting head with the same dimensions as the bars described earlier. It turned out that this is a very impractical type of mould: the casting always broke into several pieces, and pouring white-hot molten iron into the cold steel mould caused it to distort

Table IV Annealing of irregularly-shaped pieces broken from large rectangular white-cast iron plates, 400 × 100 × 2.5-4.2 mm, as described in the text, section 5. Sections for metallographic examination were cut at the thickest and thinnest part of each sample.

All samples were held at 400°C for 29 hours, then transferred to two pre-heated ovens at 850°C and 950°C respectively; held at temperature for either 68 hours (3 days) or 138 hours (6 days); then cooled in air.

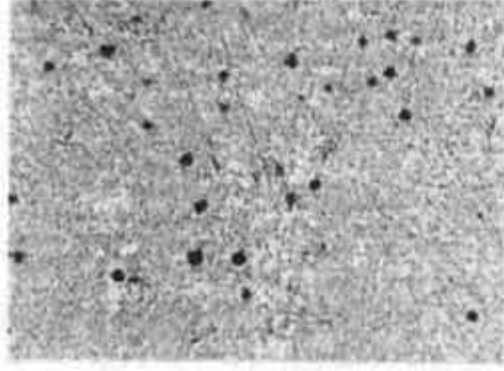
Except in the case of sample 902, all graphite nodules were compact aggregates.

Sample no.	Si %	annealing temperature, °C	annealing time, days	section thickness, mm	nodules / mm ²	diameter of largest nodule, µm	graphitized skin, µm	notes
801	0.12	850	3	2.7	0	—	10	
				3.5	0	—	10	
802	"	950	3	3.0	0	—	25	
				4.2	0.05	100	50	
803	"	850	6	2.8	0	—	30	
				4.2	0	—	50	
804	"	950	6	2.8	0.1	100	25	
				3.4	0.4	100	25	
901	0.18	850	3	2.7	0	—	20	
				3.8	0	—	0	
902	"	950	3	2.5	21.6	50	50	Spherulitic graphite; Nearly spherulitic graphite; decarburized skin.
				4.2	3.9	50	—	
903	"	850	6	2.9	0	—	20	Decarburized skin.
				4.2	0	—	—	
904	"	950	6	2.8	4.3	100	70	
				3.3	3.1	150	100	



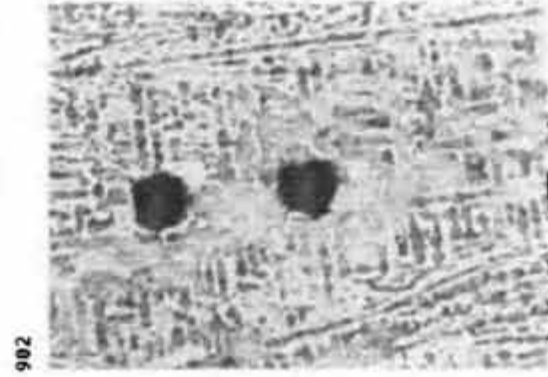
0.2 mm

2.5 mm

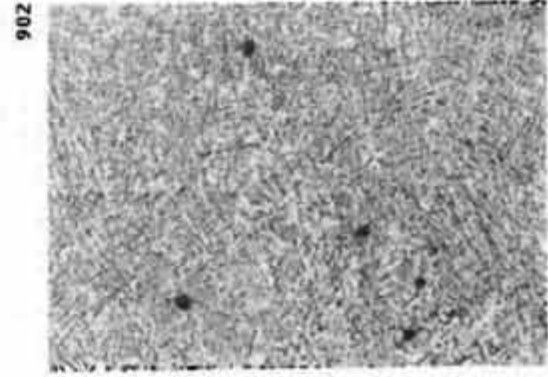


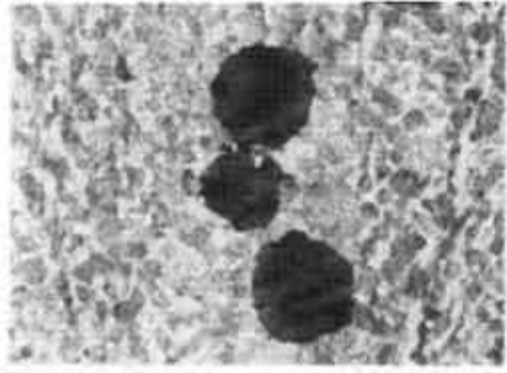
1.0 mm

Figure 22 (both pages) Micrographs from sample 902 at two different magnifications; see Table IV. Above: thinnest part of sample; below: thickest part of sample. Etched with nital.



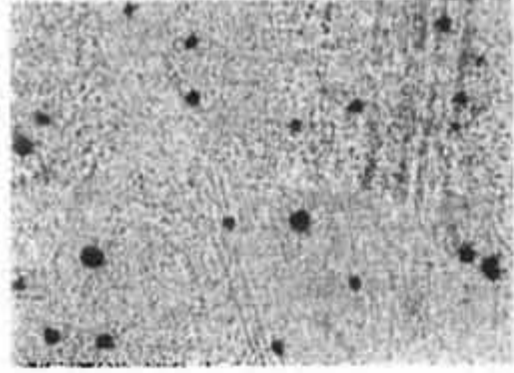
4.2 mm





904

0.2 mm



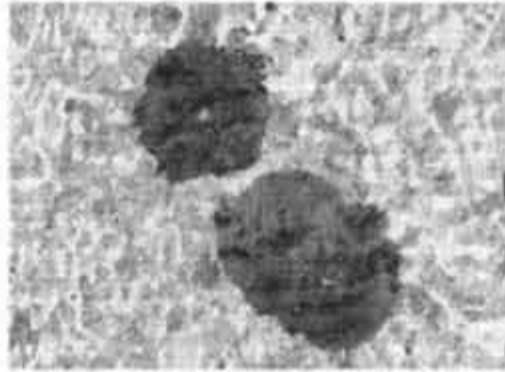
904

1.0 mm

2.8
mm

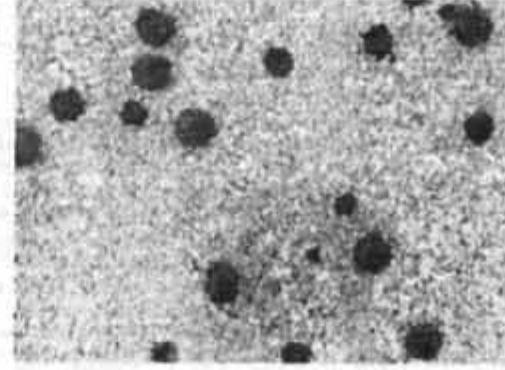
Figure 23 (both pages) Micrographs from sample 904 at two different magnifications; see Table IV. Above: thinnest part of sample; below: thickest part of sample. Etched with nitric.

904



3.3
mm

904



considerably. The samples used, broken from the cast plates, varied in thickness from 2.5 to 4.2 mm. After annealing, sections for metallographic examination were cut from the thinnest and thickest part of each sample.

The experiments reported in Table IV were intended to test the effect of section thickness (and therefore solidification rate) on first-stage graphitization. Irregularly shaped samples broken from the cast-iron plates described above were held at 400°C for 29 hours; then at either 850°C or 950°C for either 3 or 6 days; then cooled in air. Some of the resulting structures are shown in figures 22–23. Again a heavily graphitized skin was observed in all sections examined, except in two which had been “burned” by air leakage in the annealing pots.

In all but one case the extent of nucleation was less than that in the corresponding sample in Table III. In this one case, no. 902, a very surprising phenomenon was observed. In both the thin and the thick section the number of nodules was much greater than that in sample no. 612 in Table III, which was annealed in the same way. In the thin section of sample no. 902 the number of nodules was almost the largest observed in any of the experiments. Furthermore the graphite was almost spherulitic in the thick section and perfectly spherulitic in the thin section; see figure 22.

To my knowledge this phenomenon has not been observed before in scientific studies of graphite morphology in cast iron. In this iron the Mn/S ratio is 2.15, and therefore spherulitic graphite by annealing should not be expected (cf. section 4.4 above). Further research leading from this observation may help toward an understanding of how spherulitic graphite was produced in ancient Chinese blackheart malleable castings.

The most obvious features of sample no. 902 are that it is the thinnest of all the samples in the experiments, and that nucleation and growth of spherulitic graphite were greater in the thinner section from it. A hypothesis which may be worth consideration is that graphite nucleation decreases with increasing cooling rate until some critical rate is reached, whereafter it increases drastically; and that very high cooling rates also bring about graphite growth conditions which favour *c*-axis growth (spherulitic graphite) and/or retard *a*-axis growth.

It has been mentioned earlier (section 4) that different types of nucleus can be accompanied by different growth conditions for graphite. It is a common and apparently reasonable (but unproved) assumption that graphite growth is influenced only by the annealing temperature and the chemical content of the iron. Therefore it may be suspected that part of a key to an understanding of the above obser-

vation lies in an examination of the phase relations of iron, silicon, manganese, sulphur, phosphorous, and other alloying elements. For example, rapid cooling of the melt may lead to a non-equilibrium state in which certain elements (e.g. Mn, S) are in solution in the iron instead of in free inclusions. It may be that reactions take place during the long warm-up at 400°C which are analogous to those involved in the precipitation hardening of aluminium. These reactions might result in specific sub-microscopic nuclei surrounded by iron with non-typical chemical content.

In this connection attention should be drawn to a remark by the American metallurgist H. A. Schwartz in a comment on a paper by H. Morrogh (1941: 270–271): “Carbon nodules of the ‘spherulite’ type were habitually observed in the blackheart graphitizing process if that process were conducted below A_1 [723°C] or if the white cast iron had been prequenched before graphitisation.” H. Morrogh disagreed with this statement, and apparently this is where the question still rests almost fifty years later. This difference in two eminent metallurgists’ observations may be related to differences in typical compositions of American and British melting stock at the time. If it is true that pre-anneal quenching can in some cases lead to spherulitic graphite, the reason may perhaps be related to the reason for the observation reported here.

6. Acknowledgments

The research reported here is made possible by support from the Danish Research Council for the Humanities, the Carlsberg Foundation, and the University of Copenhagen. A grant for laboratory expenses was provided by Dr. Joseph Needham. The Department of Metallurgy of the Technical University of Denmark has been very generous in allowing me the use of its facilities, and Dr. V. F. Buchwald, lecturer in metallurgy, has provided both guidance and inspiration in all phases of the work. Edith Johannsen, Annelise Steffensen, Mogens Keller, and the rest of the laboratory and workshop staff have given much practical help and advice. Dr. H. Morrogh, Director of the British Cast Iron Research Association, kindly gave me detailed comments on an earlier draft of this paper. None of the persons mentioned has seen this revised version; errors and misunderstandings which remain are entirely my own responsibility. Many thanks to all.

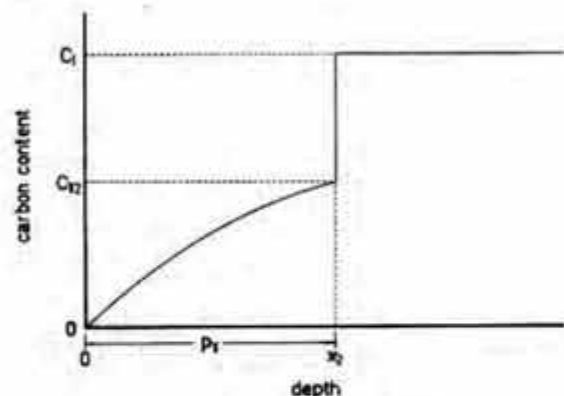


Figure 24 Variation of carbon content with depth in a plate of whiteheart malleable cast iron annealed at a temperature in the range $910^{\circ}\text{C} \leq T < 1147^{\circ}\text{C}$.

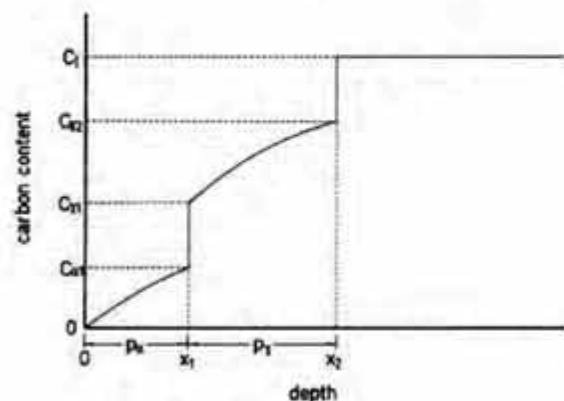


Figure 25 Variation of carbon content with depth in a plate of whiteheart malleable cast iron annealed at a temperature in the range $723^{\circ}\text{C} < T < 910^{\circ}\text{C}$.

7. Appendix: Calculation of the annealing parameters for whiteheart malleable cast iron artifacts

A thick plate of white cast iron is annealed at temperature T for time t in an atmosphere whose oxidation potential is such that the equilibrium carbon content at the surface of the iron is 0. Carbon diffuses to the surface and is oxidized, but the iron is not oxidized. At any time $t > 0$, if the temperature is in the range $910^{\circ}\text{C} \leq T < 1147^{\circ}\text{C}$, the variation of carbon content with depth in the plate will be as shown in figure 24; if $723^{\circ}\text{C} < T < 910^{\circ}\text{C}$, the variation will be as shown in figure 25.

In figures 24 and 25,

$C_{\alpha 1}$ = maximum carbon content of ferrite at temperature T .

C_{η} = minimum carbon content of austenite at temperature T .

C_{γ} = maximum carbon content of austenite at temperature T .

C_1 = initial carbon content of the white cast iron plate.

In the derivation below the dimensions of these quantities will be taken to be atoms/cm³. In the few cases in which it is necessary to refer to actual numerical values, however, these will be given as weight percentages.

Figure 26 shows how values of $C_{\alpha 1}$, C_{η} , and C_{γ} are read off from the iron-carbon phase diagram.

The sharp boundary between the ferrite and austenite zones, shown at x_1 in figure 25, is a theoretical necessity as well as an empirical fact. The sharp boundary between the austenite and ledeburite zones at x_2 in figures 24–25 is *not* a theoretical necessity, since ledeburite is a two-phase structure, but it has been found empirically that this boundary is also very sharp.

For any time $t > 0$ define

$$p_{\alpha} = x_1 = \text{thickness of ferrite layer}$$

$$p_{\gamma} = x_2 - x_1 = \text{thickness of austenite layer}$$

as shown in figures 24–25. The object of the following is to show that

$$p_{\alpha} = K_{\alpha} \sqrt{t}$$

$$p_{\gamma} = K_{\gamma} \sqrt{t}$$

where K_{α} and K_{γ} are functions of the temperature T and the initial carbon content C_1 only; and to calculate values of K_{α} and K_{γ} for the temperature range of interest.

54 East Asian Institute, Occasional Papers

For $t > 0$, $0 < x < x_2$, $x \neq x_1$, define $C(x, t)$ = carbon content at depth x and time t , atoms/cm³.

We shall in the following state and solve a system of partial differential equations for C . The statement of the equations owes a great deal to P. N. Hansen's work (1977: 32-33) on diffusion of zinc in copper.

For any time $t > 0$ define

$$\xi_{\alpha 0} = \lim_{x \rightarrow 0^+} \frac{\partial C}{\partial x} = \text{gradient of carbon content in ferrite at } x = 0$$

$$\xi_{\alpha 1} = \lim_{x \rightarrow x_1^-} \frac{\partial C}{\partial x} = \text{gradient of carbon content in ferrite at } x = x_1$$

$$\xi_{\gamma 1} = \lim_{x \rightarrow x_1^+} \frac{\partial C}{\partial x} = \text{gradient of carbon content in austenite at } x = x_1$$

$$\xi_{\gamma 2} = \lim_{x \rightarrow x_2^-} \frac{\partial C}{\partial x} = \text{gradient of carbon content in austenite at } x = x_2$$

Finally define

 D_{α} = diffusion constant for carbon in ferrite at temperature T , cm²/sec

 D_{γ} = diffusion constant for carbon in austenite at temperature T , cm²/sec

These are computed by the standard formula (see e.g. Van Vlack 1964: 104-106):

$$D = D_0 e^{-Q/RT}$$

where T is in °K and

$$D_{\alpha 0} = 0.0079 \text{ cm}^2/\text{sec}$$

$$Q_{\alpha} = 18,100 \text{ cal/mol}$$

$$D_{\gamma 0} = 0.21 \text{ cm}^2/\text{sec}$$

$$Q_{\gamma} = 33,800 \text{ cal/mol}$$

$$R = 1.987 \text{ cal/mol} \cdot ^\circ\text{K}$$

7.1. The case $910^\circ\text{C} \leq T < 1147^\circ\text{C}$. When the temperature T is in the range in which ferrite cannot occur, the variation of carbon content with depth at any time $t > 0$ is as shown in figure 24, and $\xi_{\alpha} = \xi_{\gamma} = 0$. The system of equations to be solved is, for $t > 0$ and $0 < x < x_2$:

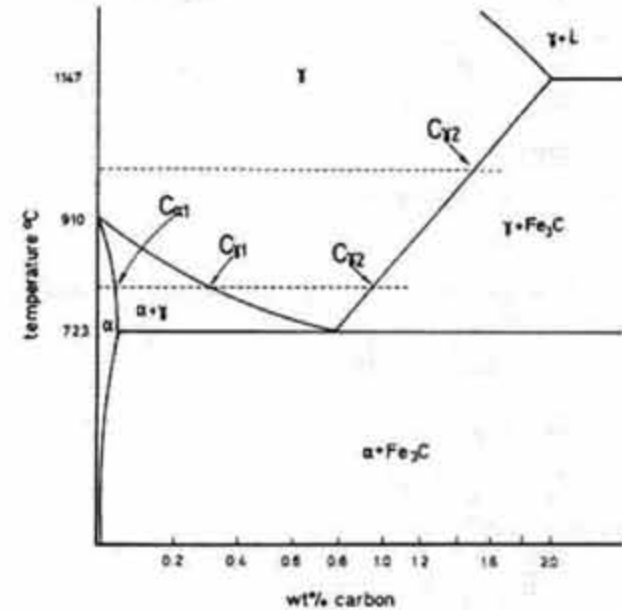


Figure 26 The lower left corner of the iron-carbon phase diagram, with indications of $C_{\alpha 1}$, $C_{\gamma 1}$, and $C_{\gamma 2}$ for two temperatures, one in the ferrite-austenite range ($723^\circ\text{C} < T < 910^\circ\text{C}$) and one in the austenite range ($910^\circ\text{C} \leq T < 1147^\circ\text{C}$). In the austenite range $C_{\alpha 1} = C_{\gamma 1} = 0$.

$$(1) \quad \frac{\partial C}{\partial t} = D_1 \frac{\partial^2 C}{\partial x^2} \quad (\text{Fick's Second Law})$$

$$(2) \quad \frac{dR_1}{dt} = \frac{D_1 g_1}{C_1 - C_2} \quad (\text{From Fick's First Law})$$

with the boundary conditions:

$$(3) \quad \lim_{x \rightarrow 0^+} C(x, t) = 0$$

$$(4) \quad \lim_{x \rightarrow x_1^-} C(x, t) = C_2$$

$$(5) \quad \lim_{t \rightarrow 0^+} R_1(t) = 0$$

I claim that the solution of (1)-(5) is:

$$(6) \quad C(x, t) = C_2 f\left(\frac{x}{R_1}\right)$$

where the function $f: [0, 1] \rightarrow [0, 1]$ is to be determined below. It follows from (6) that

$$(7) \quad \frac{\partial C}{\partial t} = -C_2 \frac{x}{R_1^2} f' \left(\frac{x}{R_1}\right) \frac{dR_1}{dt}$$

$$(8) \quad \frac{\partial C}{\partial x} = C_2 \frac{1}{R_1} f' \left(\frac{x}{R_1}\right)$$

$$(9) \quad \frac{\partial^2 C}{\partial x^2} = C_2 \frac{1}{R_1^2} f'' \left(\frac{x}{R_1}\right)$$

Substituting (7) and (9) into (1) gives

$$\frac{f'' \left(\frac{x}{R_1}\right)}{f' \left(\frac{x}{R_1}\right)} = -\frac{x}{D_1} \frac{dR_1}{dt}$$

Let

$$(10) \quad w = \frac{x}{R_1}$$

Then

$$(11) \quad \frac{f''(w)}{f'(w)} = -\frac{w R_1}{D_1} \frac{dR_1}{dt}$$

Substituting $w = 1$ gives

$$\frac{dR_1}{dt} = -D_1 \frac{f''(1)}{f'(1)} = \text{const}$$

Define K_1 such that

$$(12) \quad \frac{dR_1}{dt} = \frac{K_1^2}{2}$$

Integrating this and using (5) gives

$$(13) \quad R_1 = K_1 \sqrt{t}$$

This is the equation which we wish to prove. It has now been shown that (13) follows from the proposed solution (6), and the following will show that (6) is indeed a solution of the equations (1)-(5).

From (13) follow two useful results:

$$(14) \quad \frac{dR_1}{dt} = \frac{K_1}{2\sqrt{t}}$$

$$(15) \quad \frac{dR_1}{dt} = \frac{K_1^2}{2R_1}$$

Substituting (12) into (11) and integrating gives, for $0 \leq w \leq 1$,

$$\int_0^w \frac{f''(w)}{f'(w)} dw = -\frac{K_1^2}{2D_1} \int_0^w w dw$$

$$\log \frac{f'(w)}{f'(0)} = -\frac{K_1^2 w^2}{4D_1}$$

$$(16) \quad f'(w) = f'(0) e^{-K_1^2 w^2 / 4D_1}$$

Integrating (16) and using (3) and (4),

$$f'(0) \int_0^1 e^{-K_1^2 w^2 / 4D_1} dw = \int_0^1 f'(w) dw = 1$$

$$(17) \quad f'(0) = \frac{1}{\int_0^1 e^{-K_1^2 w^2 / 4D_1} dw}$$

Integrating (16) and using (17) and (6), the following expression for C can now be arrived at:

$$(18) \quad C(x, t) = \frac{\int_0^{x/K_1\sqrt{t}} e^{-K_1^2 w^2 / 4D_1} dw}{\int_0^1 e^{-K_1^2 w^2 / 4D_1} dw} C_2$$

It is straightforward to confirm that (18) satisfies (1), (3), (4), and (5).

Up to this point equation (2) has not been used. It will now be used to solve for K_Y . Proof that K_Y exists will complete the proof of (13). Define

$$(19) \quad G_T = \frac{e^{-K_Y^2/4D_T}}{\int_0^1 e^{-K_Y^2 w^2/4D_T} dw}$$

(Note that G_T is a constant dependent only on the temperature T and the initial carbon content C_1 .)

From (8), (16), (17), and (19),

$$(20) \quad S_T = G_T \frac{C_T}{R}$$

Substituting (15) and (20) into (2) gives

$$(21) \quad K_Y^2 = 2 D_T \frac{C_T}{C_1 - C_T} G_T$$

Equations (19) and (21) can be solved numerically for K_Y by successive approximations. We solve for the dimensionless quantity

$$X_Y = \frac{K_Y}{2\sqrt{D_T}}$$

from which it is trivial to calculate K_Y .

Substituting this and (19) into (21) gives, after some manipulation,

$$(22) \quad \frac{e^{-X_Y^2}}{2 X_Y} \frac{C_T}{C_1 - C_T} - \int_0^{X_Y} e^{-w^2} dw = 0$$

It is straightforward to solve this equation numerically using a programmable pocket calculator which has a built-in algorithm for finding roots of an arbitrary function programmed by the user. (I used a Hewlett-Packard 34C.)

The definite integral in (22) is calculated using the Taylor series:

$$(23) \quad \int_0^x e^{-w^2} dw = \sum_{n=0}^{\infty} (-1)^n \frac{x^{2n+1}}{(2n+1)n!}$$

In the range of values in which this is used here the problem of lost precision due to slow convergence does not arise.

C_1 and C_T occur in (22) only in a dimensionless ratio. Therefore, using the standard assumption of constant mass density, atomic percentages can be substituted for atomic densities with the inconvenient dimensions atoms/cm³.

C_T is not known in detail (M. Hansen 1958: 358), but it can be estimated with sufficient accuracy for present purposes by assuming that it is approximately linear between the known end-points 3.61 at% at 723°C, 8.91 at% at 1147°C. This gives

$$(24) \quad C_T = \frac{8.91 - 3.61}{1147 - 723} (T - 723) + 3.61 = 0.0125 T - 5.43 \text{ at\%}$$

The value of C_T calculated using this approximation is between 0 and 4% greater than Hansen's hypothetical curve in the entire range 723°C ≤ T ≤ 1147°C. Calculation using varying values of C_T in the range 910°C ≤ T ≤ 1050°C indicates that a variation of ± 10% in C_T gives a variation never more than 7% in the calculated values of K_Y .

A useful initial approximation for X_Y is

$$X_Y^2 = -\frac{3}{4} + \frac{1}{4} \sqrt{9 + 12 \frac{C_T}{C_1 - C_T}}$$

This approximation was derived by assuming that $C(x,t)$ can be approximated by a cubic in x for any $t > 0$. Then $\frac{\partial^2 C}{\partial x^2}$ and $\frac{\partial C}{\partial t}$ are linear in x and can be approximated by deriving limiting values of $\frac{\partial C}{\partial t}$ as $x \rightarrow 0+$ and as $x \rightarrow x_2-$. Two integrations and a good deal of tedious manipulation result in the above expression.

Figure 8 shows values of K_Y calculated by this method of successive approximations for various temperatures and for initial carbon content $C_1 = 4.3$ wt% and 3.8 wt%. These values are also tabulated in Table V, but it should be noted that the precision of these calculated values is fictive. Most of the physical constants which enter into the calculation are known to only two significant digits. Values of K_Y can be read off from figure 8 to a precision which is sufficient for all practical historians' purposes.

7.2. The case 723°C < T < 910°C. When the temperature T is in the range in which both ferrite and austenite can occur, the variation of carbon content is as shown in figure 25. The system of equations to be solved is, for $t > 0$, $0 < x < x_2$, $x \neq x_1$:

$$(25) \quad \frac{\partial C}{\partial t} = \begin{cases} D_\alpha \frac{\partial^2 C}{\partial x^2} & \text{if } 0 < x < x_1 \\ D_\gamma \frac{\partial^2 C}{\partial x^2} & \text{if } x_1 < x < x_2 \end{cases}$$

$$(26) \quad \frac{d p_\alpha}{dt} = \frac{D_\alpha g_\alpha - D_\gamma g_\gamma}{C_{\gamma 1} - C_{\alpha 1}}$$

$$(27) \quad \frac{d p_\gamma}{dt} = \frac{D_\gamma g_\gamma - d p_\alpha}{C_1 - C_{\gamma 2} - \frac{d p_\alpha}{dt}}$$

with the boundary conditions

$$(28) \quad \lim_{x \rightarrow 0^+} C(x, t) = 0$$

$$(29) \quad \lim_{x \rightarrow x_1^-} C(x, t) = C_{\alpha 1}$$

$$(30) \quad \lim_{x \rightarrow x_1^+} C(x, t) = C_{\gamma 1}$$

$$(31) \quad \lim_{x \rightarrow x_2^-} C(x, t) = C_{\gamma 2}$$

$$(32) \quad \lim_{t \rightarrow 0^+} p_\alpha(t) = 0$$

$$(33) \quad \lim_{t \rightarrow 0^+} p_\gamma(t) = 0$$

The solution of these equations follows the same general method as for the previous case, but the manipulations are much more tedious. In the following only a few of the most important intermediate results are given.

I claim that the solution of (25)–(33) above is

$$(34) \quad C(x, t) = \begin{cases} C_{\alpha 1} f_\alpha \left(\frac{x}{p_\alpha} \right) & \text{if } 0 < x < x_1 \\ C_{\gamma 1} + (C_{\gamma 2} - C_{\gamma 1}) f_\gamma \left(\frac{x - p_\alpha}{p_\gamma} \right) & \text{if } x_1 < x < x_2 \end{cases}$$

where the functions $f_\alpha, f_\gamma: [0, 1] \rightarrow [0, 1]$ are to be determined below.

From (25), (34), (32), and (33) follow

$$(35) \quad p_\alpha = K_\alpha \sqrt{t}$$

$$(36) \quad p_\gamma = K_\gamma \sqrt{t}$$

where K_α and K_γ are constants dependent only on the temperature T and the initial carbon content C_1 .

From the above the following can be derived:

$$(37) \quad f_\alpha'(w) = \frac{e^{-K_\alpha^2 w^2 / 4D_\alpha}}{\int_0^1 e^{-K_\alpha^2 w^2 / 4D_\alpha} dw}$$

$$(38) \quad f_\gamma'(w) = \frac{e^{-K_\alpha K_\gamma w / 2D_\gamma - K_\gamma^2 w^2 / 4D_\gamma}}{\int_0^1 e^{-K_\alpha K_\gamma w / 2D_\gamma - K_\gamma^2 w^2 / 4D_\gamma} dw}$$

It is straightforward to integrate these functions, derive an expression for $C(x, t)$, and confirm that (25) and (28)–(33) are satisfied. Equations (26) and (27) have not yet been used. They will now be used to solve for numerical values of K_α and K_γ . Define

$$(39) \quad G_{\alpha 1} = \frac{e^{-K_\alpha^2 / 4D_\alpha}}{\int_0^1 e^{-K_\alpha^2 w^2 / 4D_\alpha} dw}$$

$$(40) \quad G_{\gamma 1} = \frac{1}{\int_0^1 e^{-K_\alpha K_\gamma w / 2D_\gamma - K_\gamma^2 w^2 / 4D_\gamma} dw}$$

$$(41) \quad G_{\gamma 2} = G_{\gamma 1} e^{-K_\alpha K_\gamma / 2D_\gamma - K_\gamma^2 / 4D_\gamma}$$

Then from (34), (37), and (38),

$$(42) \quad g_\alpha = G_{\alpha 1} \frac{C_{\alpha 1}}{p_\alpha}$$

$$(43) \quad g_\gamma = G_{\gamma 1} \frac{C_{\gamma 2} - C_{\gamma 1}}{p_\gamma}$$

$$(44) \quad g_\gamma = G_{\gamma 2} \frac{C_{\gamma 2} - C_{\gamma 1}}{p_\gamma}$$

Substituting (42)–(44) into (26)–(27) and manipulating further gives

$$(45) \quad \frac{K_\alpha}{2} = \frac{D_\alpha G_{\alpha 1}}{K_\alpha} \frac{C_{\alpha 1}}{C_{\gamma 1} - C_{\alpha 1}} - \frac{D_\gamma G_{\gamma 1}}{K_\gamma} \frac{C_{\gamma 2} - C_{\gamma 1}}{C_{\gamma 1} - C_{\alpha 1}}$$

$$(46) \quad \frac{K_\gamma}{2} = \frac{D_\gamma G_{\gamma 1}}{K_\gamma} \frac{C_{\gamma 2} - C_{\gamma 1}}{C_1 - C_{\gamma 2}} - \frac{K_\alpha}{2}$$

The system of equations (39)–(41), (45)–(46) can be solved numerically by a method of successive approximations. We solve for the dimensionless quantities

$$X_\alpha = \frac{K_\alpha}{2\sqrt{D_\gamma}}$$

$$X_\gamma = \frac{K_\gamma}{2\sqrt{D_\gamma}}$$

from which it is trivial to calculate K_α , K_γ .

Straightforward manipulation gives the following equations, which are easier to deal with than (45)–(46):

$$(47) \quad X_\gamma^2 = S_{\alpha 1} G_{\alpha 1} + S_{\gamma 1} G_{\gamma 1} + S_{\gamma 2} G_{\gamma 2} \\ - \sqrt{(S_{\alpha 1} G_{\alpha 1} + S_{\gamma 1} G_{\gamma 1})^2 + 2 S_{\alpha 1} S_{\gamma 2} G_{\alpha 1} G_{\gamma 2}}$$

$$(48) \quad X_\alpha = \frac{S_{\gamma 2} G_{\gamma 2} - X_\gamma^2}{X_\gamma}$$

where

$$S_{\alpha 1} = \frac{1}{4} \frac{D_\alpha}{D_\gamma} \frac{C_{\alpha 1}}{C_{\gamma 1} - C_{\alpha 1}}$$

$$S_{\gamma 1} = \frac{1}{4} \frac{C_{\gamma 2} - C_{\gamma 1}}{C_{\gamma 1} - C_{\alpha 1}}$$

$$S_{\gamma 2} = \frac{1}{2} \frac{C_{\gamma 2} - C_{\gamma 1}}{C_1 - C_{\gamma 2}}$$

More convenient forms for (39)–(41) are:

$$(49) \quad G_{\alpha 1} = \frac{X_\alpha \sqrt{\frac{D_\gamma}{D_\alpha}} e^{-D_\gamma X_\alpha^2 / D_\alpha}}{\int_0^{X_\alpha \sqrt{D_\gamma / D_\alpha}} e^{-w^2} dw}$$

$$(50) \quad G_{\gamma 1} = \frac{X_\gamma e^{-X_\alpha^2}}{\int_{X_\alpha}^{X_\alpha + X_\gamma} e^{-w^2} dw}$$

$$(51) \quad G_{\gamma 2} = G_{\gamma 1} e^{-X_\gamma^2 - 2X_\alpha X_\gamma}$$

The definite integrals in (49)–(50) are calculated using the Taylor series, (23). $C_{\gamma 2}$ is approximated using (24). $C_{\alpha 1}$ and $C_{\gamma 1}$ are read off from M. Hansen's curves (1958: 353–365).

The method used to calculate X_α and X_γ for a particular temperature T and initial carbon content C_1 is as follows.

First an initial approximation is arrived at by setting $G_{\alpha 1} = G_{\gamma 1} = G_{\gamma 2} = 1$ and calculating X_α and X_γ using (47) and (48). As can be seen from (42)–(44), this approximation is equivalent to the assumption that C is approximately a linear function of x in each of the ranges $0 < x < x_1$ and $x_1 < x < x_2$.

Approximations for $G_{\alpha 1}$, $G_{\gamma 1}$, and $G_{\gamma 2}$ are then calculated using (49)–(51), and new values of X_α and X_γ are calculated using (47)–(48). This step is repeated until each of the differences between successive values of X_α and X_γ respectively is less than the desired precision.

The successive approximations generated by this algorithm do in fact converge to give values of K_α and K_γ which satisfy (45)–(46), but I have not investigated the theoretical conditions for convergence. For each T and C_1 the calculation of K_α and K_γ to four significant digits required about three minutes of computation by a programmable pocket calculator.

Values of K_α , K_γ and K_γ/K_α for various temperatures T and two initial carbon contents C_1 are tabulated in table V and graphed in figure 8. Values of K_γ/K_α for the two values of C_1 are so close that they are represented by a single curve in figure 8.

Once again it is to be noted that the precision of the calculated values in table V is fictive, and that values of K_α , K_γ and K_γ/K_α can be read off from figure 8 to a precision which is sufficient for all practical historians' purposes.

Table V Calculated values of K_a , K_y and K_y/K_a for various temperatures T and initial carbon contents C_i .

T °C	$C_i = 4.3 \text{ wt\% (17.3 at\%)}$			$C_i = 3.8 \text{ wt\% (15.5 at\%)}$		
	K_a mm/day ^{1/2}	K_y mm/day ^{1/2}	K_y/K_a	K_a mm/day ^{1/2}	K_y mm/day ^{1/2}	K_y/K_a
730	0.2815	0.01201	0.0427	0.2974	0.01306	0.0439
740	0.2783	0.03227	0.116	0.2941	0.03500	0.119
750	0.2730	0.05702	0.209	0.2885	0.06168	0.214
760	0.2666	0.08297	0.311	0.2818	0.08966	0.318
770	0.2580	0.1137	0.441	0.2729	0.1227	0.450
780	0.2475	0.1485	0.600	0.2619	0.1601	0.611
790	0.2350	0.1885	0.803	0.2487	0.2030	0.816
800	0.2206	0.2328	1.06	0.2336	0.2504	1.07
810	0.2060	0.2778	1.35	0.2182	0.2987	1.37
820	0.1899	0.3268	1.72	0.2012	0.3514	1.75
830	0.1721	0.3813	2.22	0.1826	0.4099	2.25
840	0.1533	0.4399	2.87	0.1627	0.4728	2.91
850	0.1296	0.5058	3.90	0.1376	0.5437	3.95
860	0.1095	0.5699	5.20	0.1163	0.6126	5.27
870	0.08852	0.6395	7.22	0.09409	0.6876	7.31
880	0.06696	0.7129	10.6	0.07121	0.7668	10.8
890	0.04488	0.7921	17.7	0.04775	0.8523	17.8
900	0.02252	0.8752	38.9	0.02398	0.9420	39.3
910		0.9644			1.037	
920		1.039			1.117	
930		1.117			1.202	
940		1.200			1.292	
950		1.288			1.388	
960		1.381			1.489	
970		1.478			1.595	
980		1.582			1.707	
990		1.690			1.826	
1000		1.805			1.951	
1010		1.925			2.082	
1020		2.051			2.220	
1030		2.184			2.366	
1040		2.323			2.519	
1050		2.469			2.679	
1060		2.622			2.847	
1070		2.783			3.024	
1080		2.950			3.209	
1090		3.126			3.402	
1100		3.309			3.605	

8. References and abbreviations

- Angus, H. T. 1976 *Cast iron: Physical and engineering properties*. 2nd ed., London: Butterworth.
- Barrow, John 1804 *Travels in China: Containing descriptions, observations, and comparisons, made and collected in the course of a short residence at the Imperial Palace of Yuen-Ming-Yuen, and on a subsequent journey through the country from Peking to Canton...* London: T. Cadell & W. Davies.
- Bernstein, J. 1948 "The annealing of cast iron in hydrogen", *Journal of the Iron and Steel Institute*, May 1948, pp. 11-15.
- Boegehold, A. L. 1938 "Factors influencing annealing malleable iron", *TAPS* 46: 449-490.
- Chen Yingqi & Li Enjia 1986 陈应琪、李恩佳
初论战国中山国农业发展状况
(The development of agriculture in the state of Zhongshan in the Warring States period), *NYKG* 1986.2: 117-121 + 179.
- Cranmer-Byng, J. L. (ed.) 1962 *An embassy to China: Being the journal kept by Lord Macartney during his embassy to the Emperor Ch'ien-lung, 1793-1794*. London: Longmans.
- Davis, George C. 1898 "Malleable cast-iron: Its early history in the United States", *Journal of the American Foundrymen's Association*, 5: 263-281.
- Dawson, J. V. & Smith, L. W. L. 1956 "Pinholing in cast iron and its relationship to the hydrogen pick-up from the sand mould", *B.C.I.R.A. journal of research and development* (British Cast Iron Research Association), 6: 226-248.
- Deprez, René 1930 "Contribution à l'histoire de la fonderie de malleable au pays de Liège", pp. 105-112 in *Congrès Internationale de Fonderie, Liège 23-28 juin 1930*. Hasselt: Association Technique de Fonderie de Belgique.
- Dien, Albert E. (et al., eds.) 1985 *Chinese archaeological abstracts*, vols. 2-4 (*Monumenta archaeologica*, vols. 9-11), ed. by —, Jeffrey K. Riegel, and Nancy T. Price. 3 vols., Los Angeles: Institute of Archaeology, University of California.
- Du Fuyun 1981 杜富云
冀城汉墓出土铁器的金相鉴定
(Metallographic examination of some iron arrowheads from a Han tomb in Mancheng, Hebei), *KG* 1981.1: 77-78. Summary tr. by DBW in Dien et al. 1985, 3: 1091-1093.
- Engel, Niels 1944 *Lidt om Staal og Støbejern*. København: Danmarks Tekniske Højskole.
- Fominykh, I. P. (et al.) 1967 "Comparative effectiveness of boron-containing additives", *Russian castings production*, May 1967, 245-246. Tr. from *Liteinoe proizvodstvo*.

- FTJ = *Foundry trade journal*.
- FTJ 1973, 135: 641-644 "Genius of the Chinese founder".
- Gamol'skaya, Z. M. & Rabinovich, B. V. 1964 "Low-temperature annealing of malleable iron", *Russian castings production*, May 1964, 239-240. Tr. from *Litainoe proizvodstvo*.
- Geerts, A. J. C. 1878-83 *Les produits de la nature japonaise et chinoise ... Partie inorganique et minéralogique, contenant la description des minéraux et des substances qui dérivent du règne minérale*. Yokohama: C. Levy, vol. 1, 1878; vol. 2, 1883.
- Gilbert, G. N. J. 1954 "The ductility of whiteheart malleable cast iron" (Research report no. 377), *Journal of research and development of the British Cast Iron Research Association*, Feb. 1954, pp. 1-13.
- Grill, Johan Abraham 1772 "Om poun-xa eller nativ borax", *Kongl. Vetenskaps Akademiens handlingar* (Proceedings of the Royal Swedish Academy), 33: 321-328.
- Guan Hongye & Hua Jueming 1983 关洪野·华觉明 "Research on Han Wei spheroidal-graphite cast iron", *Foundry trade journal international*, 5.17: 89-94. Abridged version, FTJ 1983, 15: 352.
- Guédras, M. 1927-28 "La fonte malléable", *La revue de fonderie moderne*, 25 mars 1927, 30-32; 10 avril, 58-61; 25 juin, 185-190; 10 juillet, 210-213; 25 sept., 375-376; 10 nov., 443-447; 10 janv. 1928, 7-14; 25 janv., 27-29.
- Guo Moruo 1973 郭沫若 *Nulizhi shidai 奴隶制时代* (The age of slavery). 2nd ed., Beijing: Xinhua Shuju.
- Hansen, Max 1958 *Constitution of binary alloys*. 2nd ed., New York: McGraw-Hill.
- Hansen, Preben Nordgaard 1977 "Diffusionsteori", pp. 15-43 in V. F. Buchwald, ed., *Varmehandling og værktøjsfremstilling*. Bjerringbro, Denmark: Dansk Metallurgisk Selskab.
- Henger, G. W. 1970 "The metallography and chemical analysis of iron-base samples dating from antiquity to modern times", *Historical metallurgy: Journal of the Historical Metallurgy Society*, 4.2: 45-52.
- Hernandez, Abelardo 1967 "Analysis of survey on heat treatment practices used for annealing ferritic malleable castings", *TAFS* 75: 605-610.
- Honda, Kōtarō & Murakami, Takejiro 1920 "On graphitisation of iron-carbon alloys", *Journal of the Iron and Steel Institute*, 102.2: 287-294.
- Hua Jueming (et al.) 1980 华觉明 两千年前有球状石墨的铸铁 (Cast iron with spherulitic graphite from two thousand years ago), by —, Li Jinghua 李京华, Guan Hongye 关洪野, and Ji Chengzhou 吉承周. *Qiutie 球铁* (SG-iron), 1980.2: 1-8.
- 1982 试做高强度铸铁的探讨 (A discussion of the high-strength cast iron of the Han and Wei periods), *Ziran kexue shi yanjiu 自然科学史研究* (Studies in the history of natural sciences), 1.1: 1-20 + plates 1-2.
- Hultgren, Axel & Östberg, Gustaf 1954 "Structural changes during annealing of white cast irons of high S:Mn ratios: Including the formation of spherulitic and non-spherulitic graphite and changes in sulphide inclusions", *Journal of the Iron and Steel Institute*, 176: 351-365. Tr. of 1955.
- 1955 "Strukturförändringar under glödning av vita gjutjärn med hög Si:Mn-kvot, inafattande bildning av sfärolitisk och icke-sfärolitisk grafit samt förändringar i sulfidinslutningarna", *Jernkontorets annaler*, 139: 1-10.
- Hunter, M. J. & Chadwick, G. A. 1972a "Structure of spheroidal graphite", *Journal of the Iron and Steel Institute*, Feb. 1972, 117-123.
- 1972b "Nucleation and growth of spheroidal graphite alloys", *Journal of the Iron and Steel Institute*, Sept. 1972, 707-717.
- James, Charles 1900 "On the annealing of white cast iron", *Journal of the Franklin Institute* (Philadelphia), 150.3: 227-235.
- Johnson, W. C.; Kovacs, B. V.; & Clum, J. A. 1974 "Interfacial chemistry in magnesium modified nodular iron", *Scripta metallurgica*, 8: 1309-1316.
- KG = *Kaogu* 考古 ("Archaeology").
- KG 1975.4: 241-243 易县燕下都44号墓群铁器金相考察初步报告 (Preliminary report on the metallographic examination of iron artifacts from Grave no. 44 at Yanxiadu, Yixian County, Hebei), by the Pressure-Processing Section, Beijing University of Iron and Steel Technology 北京钢铁学院压力加工专业. Translation by DBW in Dien et al. 1985, 3: 849-853.
- KG 1978.6: 400-401 + plate 10 磁县元代木船出土铁器金相报告 (Metallographic analysis of iron artifacts from the Yuan-period shipwrecks found in Cixian County, Hebei), by the Chinese Archaeo-Metallurgy Study Group = 中国冶金史·编写组 and Capital Iron and Steel Company Research Institute, Metallurgy Group 首钢研究所金相组. Tr. by DBW in Dien et al. 1985, 4: 1946-1948.
- KGTX = *Kaogu tongzun* 考古通讯 (Archaeological bulletin).
- KGXB = *Kaogu xuebao* 考古学报 ("Acta archaeologica Sinica").
- KGXB 1978.1: 1-24 + plates 1-2 河南汉代冶铁技术初探 ("The iron and steel making techniques of the Han dynasty in Henan"), by the Henan Provincial Museum 河南省博物馆; the Blast Furnace Plant of the Shijingshan Steel Plant, Shoudu Iron and Steel Company 石景山钢铁公司炼铁厂; and the Chinese Archaeo-Metallurgy Study Group = 中国冶金史·编写组. English summary p. 24.

- Kikuta, Taro 1926 "On the malleable cast iron and the mechanism of its graphitization", *Science reports of the Tohoku Imperial University*, 13: 115-155.
- Kusakawa Takaji & Nakata Eichi 1963 草川隆次、中田栄一
深腐食法による鋼鉄中黒鉛の立体的観察
("Three dimensional observation of graphite in cast iron by deep etching method"), *Imono kokuho* ("Journal of the Japan Foundrymen's Society"), 35.8: 470-475. Includes English abstract.
- Li Buqing 1960 李步青
山东滕县发现铁范
(An iron mould discovered in Tengxian County, Shandong), *KG* 1960.7: 72.
- Li Chunli; Liu Baicheng; & Wu Dehai (eds.) 1983 李春立、柳百成、吴德海
Zhutie shimo tupu—Guangxue yu saomiao dianzi xianweijing zhaopian
铸铁石墨图谱—光学与扫描电子显微照片
(Cast-iron graphite album: Optical and SEM micrographs). Beijing: Jixie Gongye Chubanshe.
- Li Jinghua 1965 李京华
从南阳宛城遗址出土汉代犁铧和铁范看犁铧的铸造工艺过程
(The technical process of casting ploughshares in the light of the Han-period ploughshare models and moulds unearthed at the Wancheng site in Nanyang, Henan), by the Cultural Relics Work Team of the Henan Provincial Cultural Office 河南省文化局文物工作队; written by —, *WW* 1965.7: 1-11.
- Li Zhong 1975 李众
中国封建社会前期钢铁冶炼技术发展的探讨
("The development of iron and steel technology in ancient China"), *KGXB* 1975.2: 1-22 + plates 1-6. English summary pp. 21-22.
- Lohse, U. 1910 "Die geschichtliche Entwicklung der Eisengießerei seit Beginn des 19. Jahrhunderts", *Beiträge zur Geschichte der Technik und Industrie*, 2: 90-147.
- Loper, C. R. & Takizawa, N. 1965 "Spheroidal graphite development in white cast irons", *TAPS* 72: 520-528.
- Lu Da 1965 陆达
"Die uralte Technik der Eisenherstellung in China"
中国古代的冶铁技术
German and Chinese text, pp. 63-70 in *Vita pro ferro: Festschrift für Robert Durrer zum 75. Geburtstag am 18. November 1965*. Schaffhausen. Chinese text also in *Jinshu xuebao* 金属学报 ("Acta chemica Sinica"), 1966, 9.1: 1-3 + plates 1-4.
- Maurmann, Walther 1923 "Entstehung und Entwicklung der Tempergussindustrie im Bezirke der bergisch-märkischen Kleisenenindustrie", *Auszüge aus Doktor-Dissertationen der Rechts- und Staatswissenschaftlichen Fakultät der Georg-August-Universität zu Göttingen*, Jhrg. 1923. 4 pp. without pagination.
- Merchant, Harish D. 1961 "Solidification, structure, and properties of gray iron", *Foundry*, Nov. 1961, 80-87.
- Moldenke, Richard 1919 "Discussion—malleable iron as an engineering material", *TAPS* 27: 400-403. (Concerns the history of laboratory control in malleable foundries.)
- Moore, C. T. 1960 "Some experiments on the properties of ferritic blackheart malleable cast iron", *The British foundryman*, March 1960, pp. 107-119.
- Morrogh, H. 1941 "The polishing of cast-iron micro-specimens and the metallography of graphite flakes"; "The metallography of inclusions in cast irons and pig irons"; discussion. *Journal of the Iron and Steel Institute*, 1941 no. 1, pp. 195P-205P, 207P-253P, 254P-286P, plates XXXVIII-XLVII, XLVIA, XLVIB.
- 1955 "Graphite formation in grey cast irons and related alloys", *B.C.I.R.A. journal of research and development* (British Cast Iron Research Association), 5: 655-673.
- 1962 "Progress and problems in the understanding of cast irons", *TAPS* 70: 449-458.
- 1968 "The status of the metallurgy of cast irons", *Journal of the Iron and Steel Institute*, Jan. 1968, 1-10.
- Murthy, V.S.P.; Kishore; & Sesan, S. 1986 "Morphology of flake, ductile and compacted graphite", *Journal of metals*, 38.12: 24-28.
- NYKG = *Nongye kaogu* 农业考古 ("Agricultural archaeology").
- Ohide Taku & Ohira Goro 1970 大出卓、大平五郎
純粋系白鑄鉄の黒鉛化における焼鈍黒鉛の球状化
("Spheroidization of temper carbon in the graphitization of pure white cast iron"), *Imono kokuho* ("Journal of the Japan Foundrymen's Society"), 42.5: 394-404. Includes English abstract.
- Pinel, Maurice L.; Read, Thomas T.; & Wright, Thomas A. 1938 "Composition and microstructure of ancient iron castings", *Transactions of the American Institute of Mining and Metallurgical Engineers*, 181: 174-194. ("Issued as T.P. 882 in *Metals Technology*, January 1938".)
- Rehder, J. E. 1945 "Annealing malleable iron: Principles and practice, special processes, annealing cycles", *Canadian metals and metallurgical industries*, 8.6: 29-34.
- 1949 "Effects of temperature and silicon content on first stage annealing of black-heart malleable iron", *TAPS* 57: 173-180.
- 1951 "The relative effects of chromium and silicon on rate of anneal of black-heart malleable iron", *TAPS* 59: 244-252.
- Rein, J. J. 1881-86 *Japan nach Reisen und Studien: Im Auftrage der Königlich Preussischen Regierung dargestellt*. Vol. 1: *Natur und Volk des Mikado-reiches*, 1881. Vol. 2: *Land- und Forstwirtschaft, Industrie und Handel*, 1886. Leipzig: Wilhelm Engelmann.
- 1889 *The industries of Japan: Together with an account of its agriculture, forestry, arts, and commerce*. London: Hodder and Stoughton.
- Roll, Franz 1928 "Die Raumform des Graphits", *Gieserei*, 15.51: 1270-1274.

- Rostoker, William 1988 "The ancient heat treatment of white cast iron", pp. 200-204 in *The beginning of the use of metals and alloys*, ed. by Robert Maddin, Cambridge, Mass. & London: M.I.T. Press.
- ; Bronson, B.; & Dvorak, J. 1984 "Studies on an ancient Chinese cast-iron object with a bronze coating", *Historical metallurgy: Journal of the Historical Metallurgy Society*, 18.2: 89-94.
- Rote, F. B.; Chojnowski, E. F.; & Bryce, J. T. 1956 "Malleable base spheroidal iron", *TAPS* 64: 197-208.
- Roit, Carl 1881 "Die Fabrikation des schmiedbaren und Tempergusses", *Der praktische Maschinen-Constructeur: Zeitschrift für Maschinen- und Mühlenbauer, Ingenieure und Fabrikanten*, 40.18: 344-346; 40.19: 366-368.
- Sander, Leonard M. 1987 "Fractal growth", *Scientific American*, Jan. 1987, 256: 82-88.
- Schneidewind, Richard 1950 "A summary of the quantitative effects of some factors on the annealing of white cast iron", *TAPS* 58: 202-207.
- Schneidewind, Richard & Reese, D. J. 1949 "Influence of rate of heating on first stage graphitization of white cast iron", *TAPS* 57: 497-508.
- Schneidewind, Richard; Reese, D.J.; & Tang, A. 1947 "Graphitization of white cast iron: Effect of section size and annealing temperature", *TAPS* 55: 252-259.
- Schubert, H. R. 1957 *History of the British iron and steel industry: from c. 450 B.C. to A.D. 1775*. London: Routledge & Keagan Paul.
- Schütz, E. & Stotz, R. 1930 *Der Temperguss: Ein Handbuch für den Praktiker und Studierenden*. Berlin: Springer.
- Schwartz, H. A. 1922 *American malleable cast iron*. Cleveland, Ohio: Penton.
- Sisco, Anneliese Grünhaldt (tr.) & Smith, Cyril Stanley (ed.) 1956 *Résumé of Memoirs on iron and steel*. Chicago: University of Chicago Press.
- Sjögren, H. (tr.) 1923 *Mineralriktet, av Emanuel Swedenborg: Om järnet och de i Europa vanligast vedertagna järnframställningssätten ...* Stockholm: Wahlström & Widstrand. Tr. of Swedenborg 1734.
- Stein, E. M. (et al.) 1970 "Effects of variations in Mn and S contents and Mn-S ratio on graphite-nodule structure and annealability of malleable-base iron", *TAPS* 78: 435-442.
- Strickland, — 1826 "On softening cast iron", *The Franklin journal and American mechanics' magazine*, 2.3: 184-185. ("Extract from the reports of Mr. Strickland [just published]". The source is not given.)
- Swedenborg, Emanuel 1734 *Regnum subterraneum sive minerale*. [Vol. 2:] *De ferro, deque modis liquationum ferri per Europam passim in usum receptis ...* Dresdae et Lipsiae: sumptibus Friderici Hekelii.
- 1762 *Traité du fer*, par M. Swedenborg; trad. du Latin par M. Bouchu. (*Description des arts et métiers: Art des forges et fourneaux à fer*, par M. le Marquis de Courtivron et par M. Bouchu; 4ème section). [Paris: Guerin et Delatour]. [Réimp. Genève: Slatkine Reprints, 1984].
- TAPS = *Transactions of the American Foundrymen's Society*.

- Terhune, R. H. 1871 "Malleable cast iron", *Transactions of the American Institute of Mining Engineers*, 1: 233-239.
- Tkachenko, F. K. & Maistruk, A. Ya. 1962 "Influence of quenching on the graphitization of white iron", *Russian castings production*, May 1962, 200-203. Tr. from *Liteinoe proizvodstvo*.
- Todorov, Radoslav & Nikolov, Michail 1970 "Einfluss der Vorglühung von Temperguss auf die Menge und Verteilung der Graphitkeime über den Querschnitt", *Giesserei*, 57.8: 197-200.
- Tsutsumi, Nobuhisa & Hoshibara, Satoshi 1975 "Study on the effect of pre-baking at sub-critical temperature on the graphitization of white iron", *Report of the Castings Laboratory, Waseda University* (Tokyo), 26: 61-67.
- Van Vlack, Lawrence H. 1964 *Elements of materials science: An introductory text for engineering students*. 2nd ed., Reading Mass., etc.: Addison-Wesley.
- Vogel, Otto 1918-20 "Lose Blätter aus der Geschichte des Eisens", XI-XIV: "Zur Geschichte der Tempergusserei", *Stahl und Eisen* (1918) 38.48: 1101-1105; 38.52: 1210-1215; (1919) 39.52: 1617-1620; (1920) 40.26: 869-872.
- [Voye, Ernst] 1914 "Zur Geschichte der Tempergiesserei in der westfälischen Mark", *Die Giesserei*, 1.4: 54-55. ("Aus Dr. Ernst Voye, Geschichte der Industrie im märkischen Sauerland, 4 Bände, Hagen i. W., Otto Hamerschmidt 1908 bis 1913.")
- Wang Jiayin 1957 王嘉猷
Ben cao gang mu de kuangtou shiliao 本草綱目的矿物史料
(Materials for the history of mineralogy in Li Shizhen's *Ben cao gang mu*). Beijing: Kexue Chubanshe.
- White, A. E. & Schneidewind, R. 1933 "Effect of superheat on annealing of malleable iron", *TAPS* 41: 98-111.
- Wieser, P. F. (a.o.) 1967 *Mechanism of graphite formation in iron-carbon-silicon alloys*. Cleveland, Ohio: Malleable Founders Society.
- WW = Wenzu 文物 ("Cultural relics").
- WW 1976.8: 52-58 + plate 4
河南濬縣商周快器檢驗報告
(Metallographic examination of iron artifacts from a trove in Mianchi County, Henan), by the Department of Metal Materials and the Central Analytical Laboratory, Beijing University of Iron and Steel Technology 北京鋼鐵學院金屬材料系中心實驗室. Tr. by DBW in Dien et al. 1985, 3: 1066-1075.
- WW 1978.10: 44-48
長沙新發現春秋晚期的鋼劍和快器
(A steel sword and some iron artifacts of the late Spring and Autumn period discovered in Changsha, Hunan), by the Construction Archaeological Team of the Changsha Railway Station 長沙鐵路車站建設工程文物發掘隊. Summary translation by DBW in Dien et al. 1985, 3: 728-733.

WWCZ = Wentou cankao ziliao 文物参考资料 (Cultural relics reference materials).

Yang Gen & Ling Yejin 1962 杨根、凌业勤

中国最早的金属型 (铸铁)

(The earliest metal moulds used in China [cast iron]), *Jixie gongcheng xuebao* 机械工程学报 ("Chinese journal of mechanical engineering"), 10.3: 100-103. Very brief English abstract.

Ye Jun 1975 冶军

铜绿山古矿井遗址出土铁制及铜制工具的初步鉴定

(Preliminary metallographic examination of iron and bronze implements from the ancient mine site at Tonglushan in Daye County, Hubei), WW 1975.2: 19-25. Tr. by DBW in Dien et al. 1985, 3: 715-725.

Zhang Zigao & Yang Gen 1973 张子高、杨根

从侯马陶范和兴隆铁范看战国时代的冶铸技术

(Metallurgical techniques of the Warring States period in the light of the ceramic moulds from Houma, Shanxi and the iron moulds from Xinglong, Hebei), WW 1973.6: 62-65 + 60 + inside back cover.

Zheng Shaozong 1956 郑昭宗

热河兴隆发现的战国生产工具铸范

(Warring States period moulds for production implements discovered in Xinglong, Rehe), KGTX 1956.1: 29-35 + plates 9-10. (The province of Rehe was abolished in 1956; Xinglong is now in Hebei province.)

Zhu Huo & Bi Baoqi 1977 朱浩、毕宝琦

山东省莱芜县西汉农具铁范

(Western Han iron moulds for agricultural implements found in Laiwu County, Shandong), by the Shandong Provincial Museum 山东省博物馆. written by —, WW 1977.7: 68-73.

Zi Xi 1957 齐锡

谈几种器物的范

(On moulds for various objects), WWCZ 1957.8: 45-48.

East Asian Institute Occasional Papers

previously published

- No. 1 Symposium on Korea: Simon B. Heilesen: *Yet Another Journal*. Kirsten Gottfredsen: *The Role of Language in Modern Korean Society*. Tedda Rønnenkamp-Holst: *Socio-Cultural Aspects of the History of Korean Script*. Henrik Hjort Sørensen: *The Conflict between Buddhism and Christianity in Korea*. Olof G. Lidin: *Korean Studies in Denmark*. (1988)
- No. 2 Tonami Mamoru: *The Sui Dynasty Inspection of Countenances and the Early Tang Fiefs of Maintenance* (translated by Jens Østergård Petersen). Henrik Hjort Sørensen: *The Conflict between Son and Doctrinal Buddhism in Silla*. (1988)
- No. 3 Henrik H. Sørensen: *A Survey of the Religious Sculptures of Anyue*. (1989)

Vertical text on the left margin, possibly a page number or header.

ISSN 0903-6822